Production of nuclei and hypernuclei in relativistic ion reactions

Alexander Botvina , Marcus Bleicher

ITP, Goethe University, Frankfurt am Main , Germany

Nihal Buyukcizmeci

Selcuk University, Konya, Turkey

HYP2022 conference
(Prague, Czech Republic)
June 27-July 1, 2022

The formation of nuclear fragments in collisions of nuclei is a many-body process, there is no a dominating channel. The theoretical explanation requires both dynamical and statistical approaches.

It can be subdivided into two main stages:

1) Dynamical stage leading the production of new baryons (+ in some cases, lightest nuclei) and excited equilibrated nuclear systems, e.g., nuclear residues.

2) Statistical disassembly of these systems leading to the production of final nuclei.

Qualitative picture of dynamical stage of the reaction leading to fragment production (e.g., UrQMD calculations)

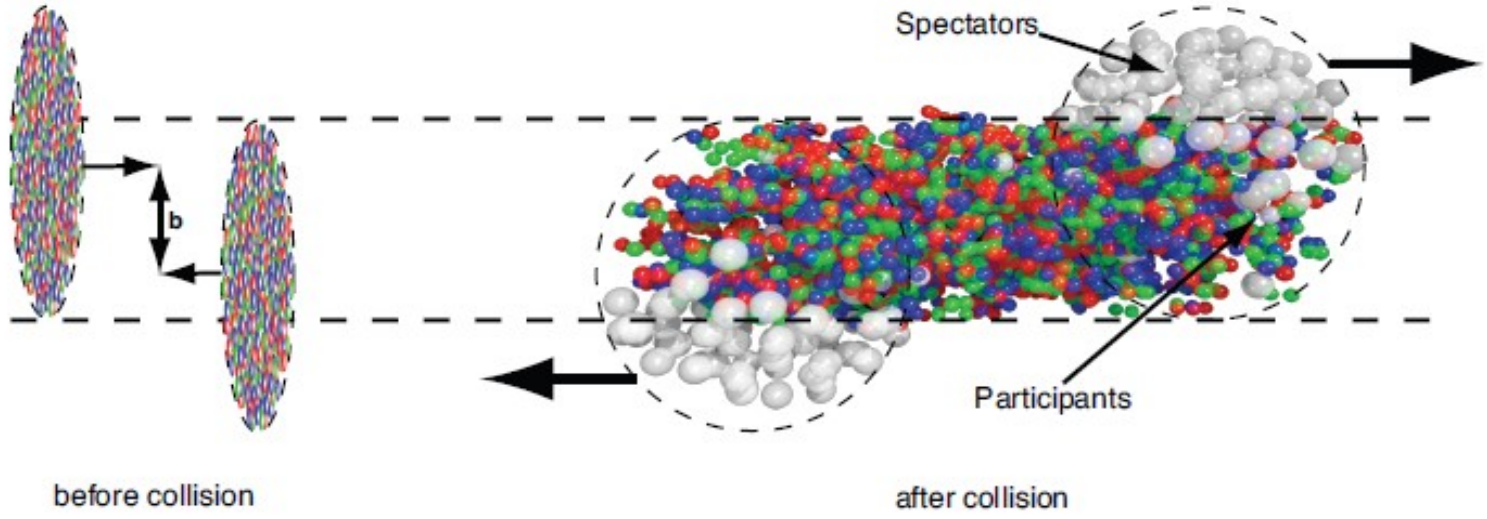

Fragment formation is possible from both participants and spectator residues

UrQMD PHSD DCM GiBUU

Production mechanisms of nuclear cluster species including anti-matter, hyper-matter in relativistic HI and hadron collisions:

- Production of all kind of particles (anti- , strange, charmed ones) in individual binary hadron collisions. Effects of nuclear medium can be included.
- Secondary interactions and rescattering of new-born particles are taken into account. (Looks as partial ‘thermalization’.)
- Nucleation process of produced baryons into composite (normal. exotic, anti- , hyper-) nuclear species.
- Capture of produced baryons by big excited nuclear residues.

Statistical decay of excited nuclear species into final nuclei

- Multifragmentation into small nuclei (high excitations),
- Evaporation and fission of large nuclei (low excitations),
- (Fermi-) Break-up of small nuclei into lightest ones.

All transport modes predict similar picture: Hyperons can be produced at all rapidities, in participant and spectator kinematic regions.

Wide rapidity distribution of produced Λ!

Calculation: DCM PRC**84**(2011)064904

S.Albergo et al., E896: PRL88(2002)062301

Au(11AGeV/c)+Au

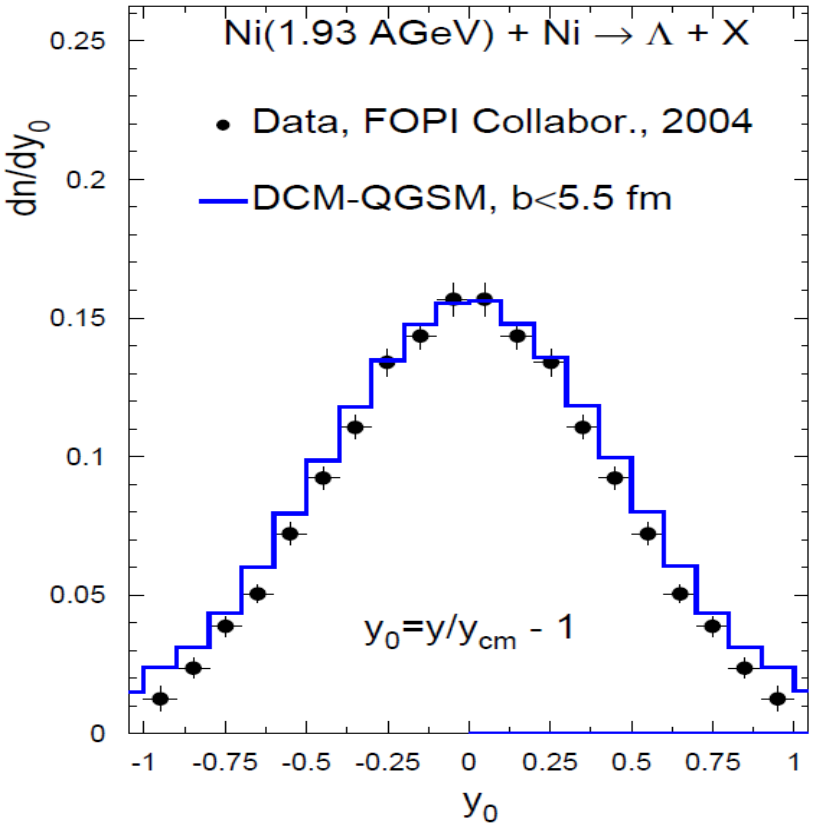

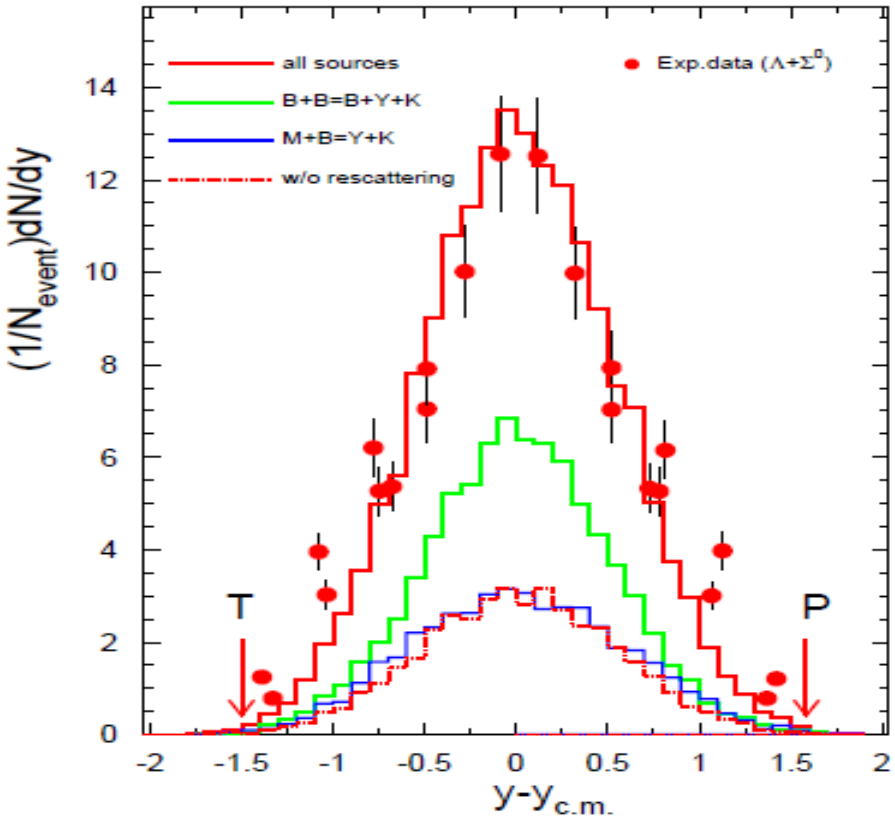

Low/intermediate energies: hadron/lepton collisions with nuclei, the same mechanisms in peripheral ion collisions

Dinamical stage with particle emission and production of excited nuclear residues

Preequlibrium emission + equilibration

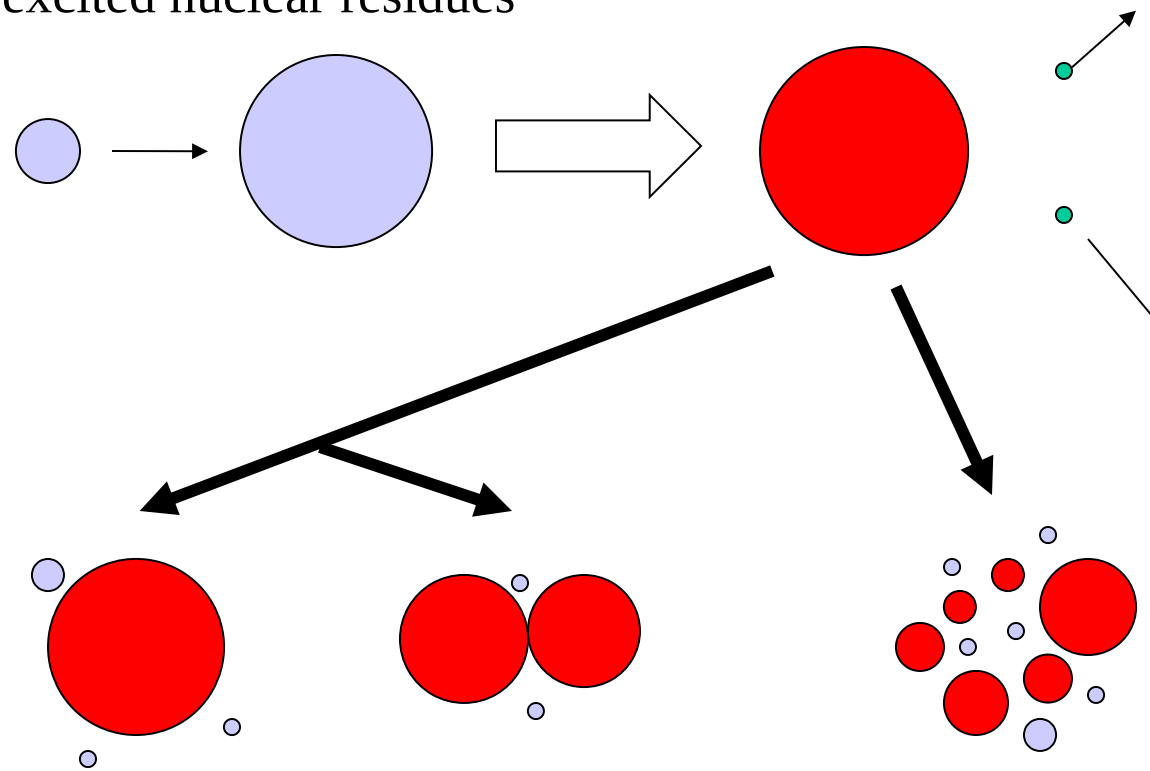

evaporation

fission

multifragmentation

Statistical approach

N.Bohr (1936)

Compound-nucleus decay channels (sequential evaporation or fission) dominate at low excitation energy of thermal sources E^*<2-3 MeV/nucl

N.Bohr, J.Wheeler (1939)
V.Weisskopf (1937)

starting 1980-th, conception: statistical freeze-out volume

At high excitation energy E^*>3-4 MeV/nucl there is a simultaneous break-up into many fragments (e.g. SMM: Phys.Rep.**257**(1995)133)

Statistical Multifragmentation Model (SMM)

J.P.Bondorf, A.S.Botvina, A.S.Iljinov, I.N.Mishustin, K.Sneppen, Phys. Rep. **257** (1995) 133

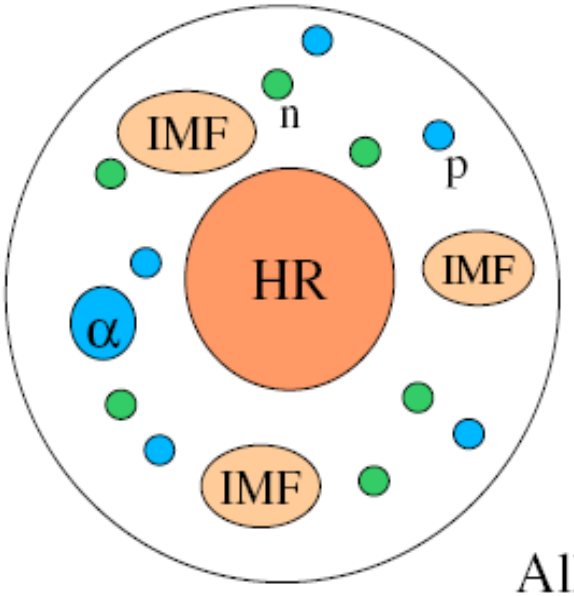

Ensemble of nucleons and fragments
in thermal equilibrium characterized by

neutron number N_0

proton number Z_0, $N_0+Z_0=A_0$

excitation energy $E^*=E_0-E_{CN}$

break-up volume $V=(1+\kappa)V_0$ freeze-out

All break-up channels are enumerated by the sets of fragment multiplicities or partitions, $f=\{N_{AZ}\}$

Statistical distribution of probabilities: $W_f \sim \exp\{S_f(A_0, Z_0, E^*, V)\}$
under conditions of baryon number (A), electric charge (Z) and energy (E*) conservation, including compound nucleus.

A.S.Botvina and J.Pochodzalla, Phys. Rev.C76 (2007) 024909

Generalization: statistical de-excitation model for nuclei with Lambda hyperons

In these reactions we expect analogy with

multifragmentation in intermediate and high energy nuclear reactions

+ nuclear matter with strangeness

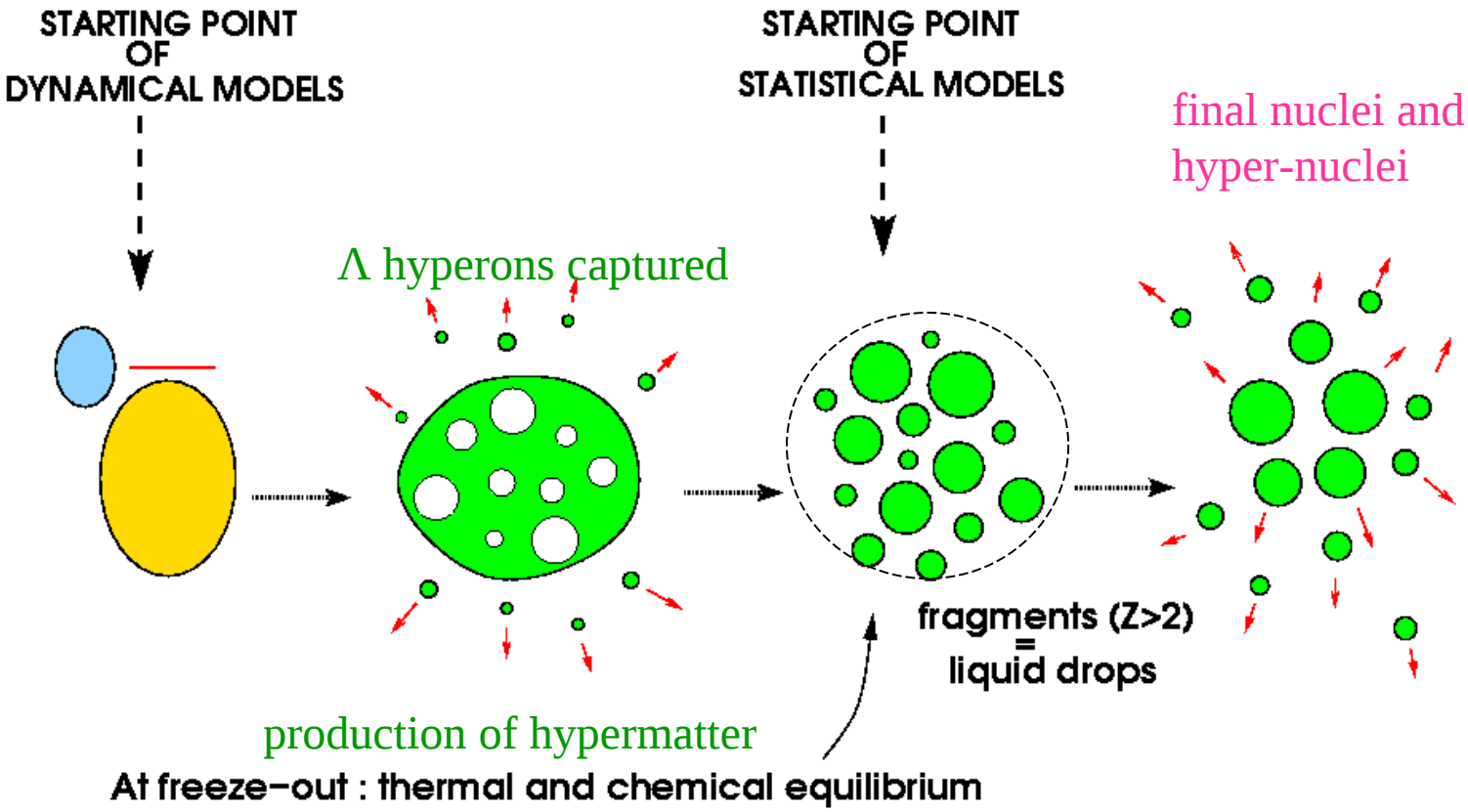

Long tradition of fragment measurements in high energy reactions:

Fragment production in Au+Au collisions: ALADIN (GSI) + Multics/Miniball (MSU) experiments

(G.J.Kunde et al., PRL 74, 38 (1995))

Difference of fragment yields obtained in spectator region (very broad distribution) and in central collisions (exponential fall of yields with mass/charge): Indication on different fragment production mechanisms.

Also there is a fragment flow in central collisions (high kinetic energies per nucleon respective to c,m, of decaying system).

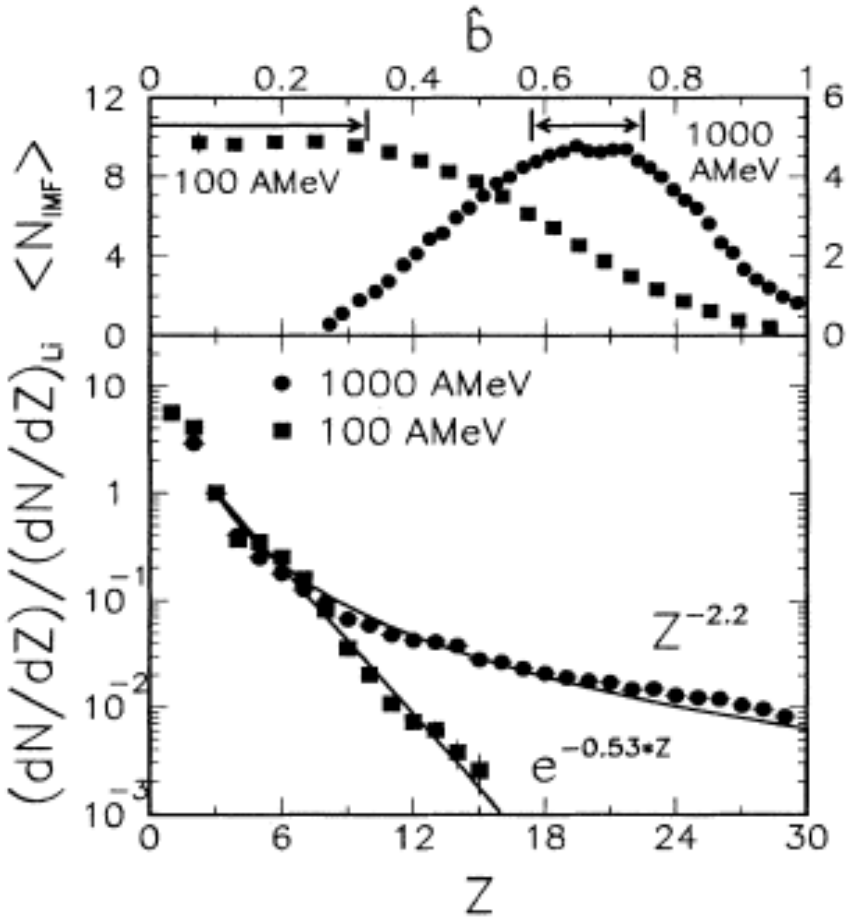

Two-stage multifragmentation of 1*A* GeV Kr, La, and Au

EOS collaboration: fragmentation of relativistic projectiles

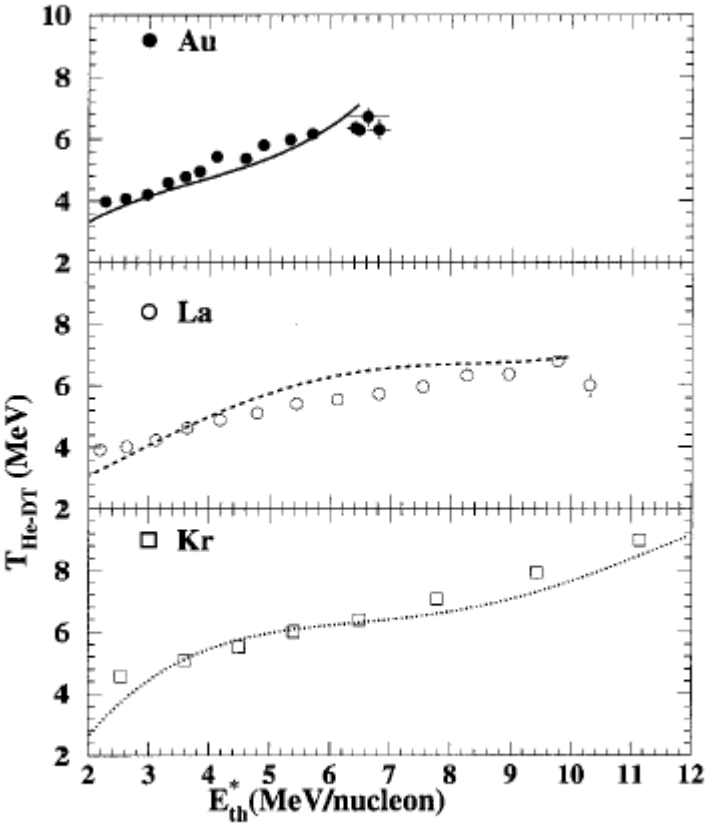

FIG. 19. Caloric curves (T_f vs E^*_{th}/A) for Kr, La, and Au. Points are experimental and curves are from SMM.

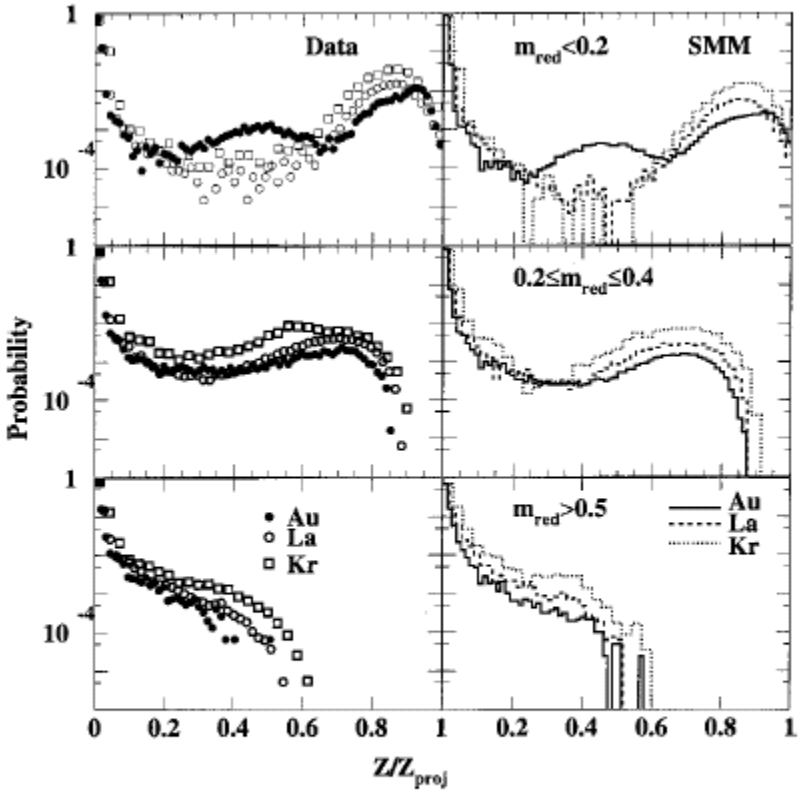

FIG. 24. Second stage fragment charge distribution as a function of $Z/Z_{\text{projectile}}$. Results are shown for three reduced multiplicity intervals for both data and SMM.

ALADIN data

GSI

multifragmentation of relativistic projectiles

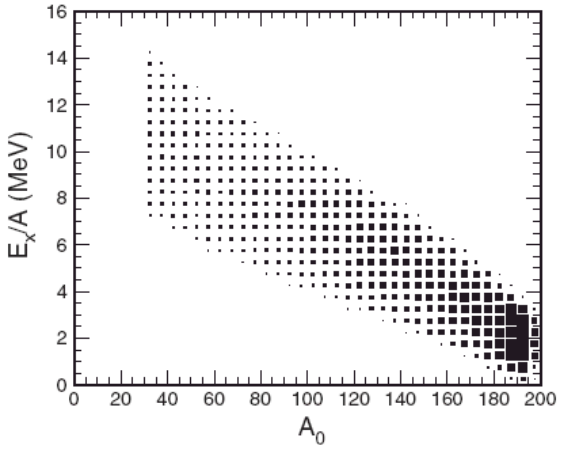

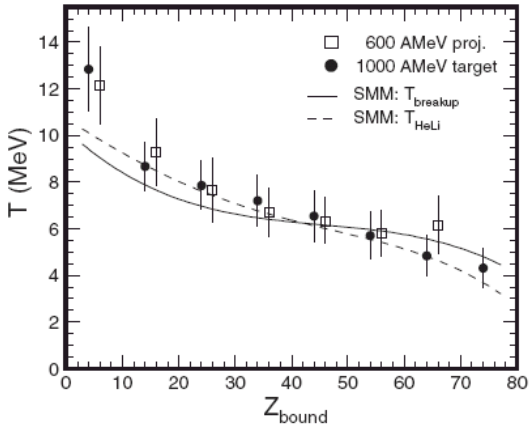

A.S.Botvina et al.,
Nucl.Phys. A584(1995)737

H.Xi et al.,
Z.Phys. A359(1997)397

comparison with SMM (statistical multifragmentation model)

Statistical equilibrium has been reached in these reactions

Au(600MeV/n)+C,Al,Cu

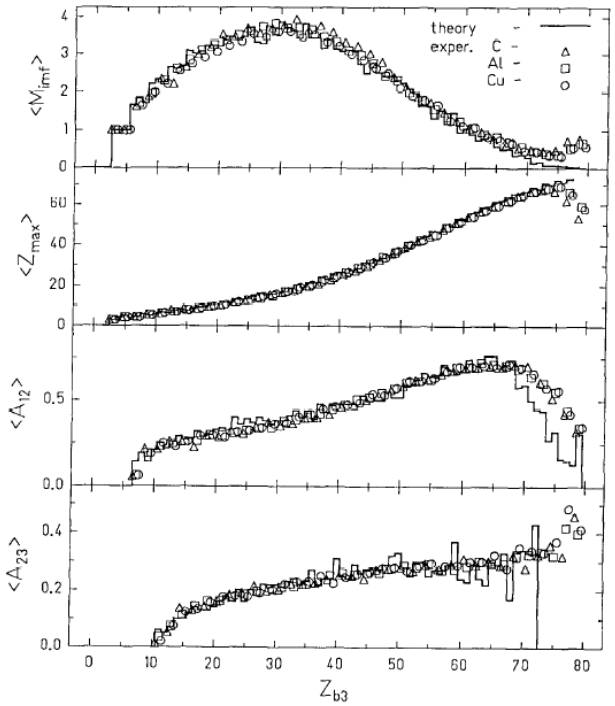

Au(600MeV/n)+Cu

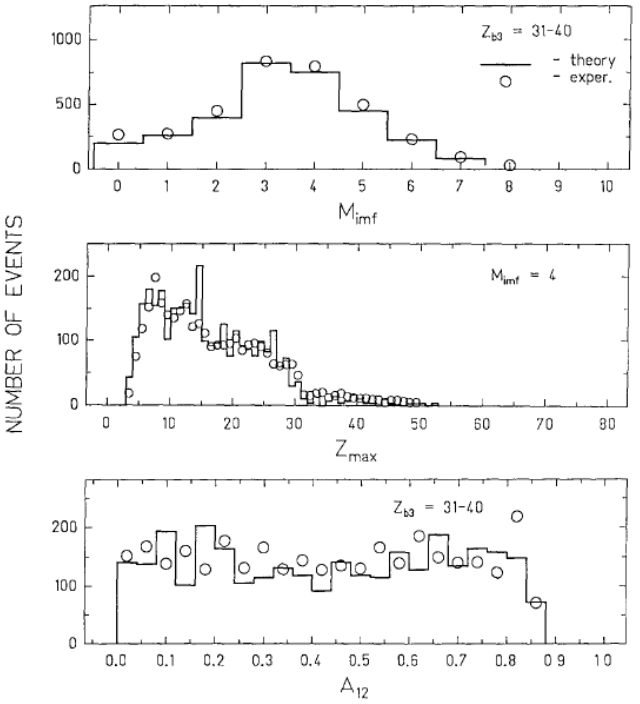

ALADIN data

GSI

multifragmentation of relativistic projectiles

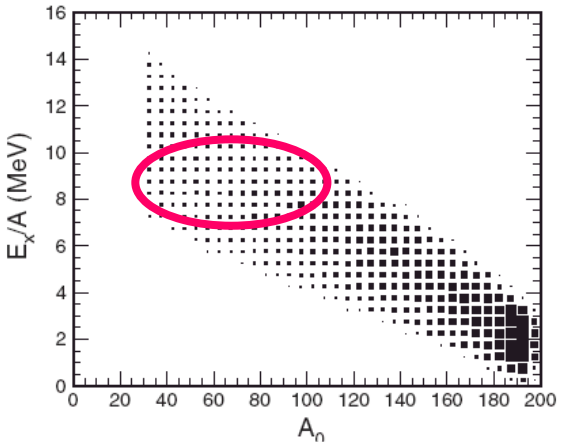

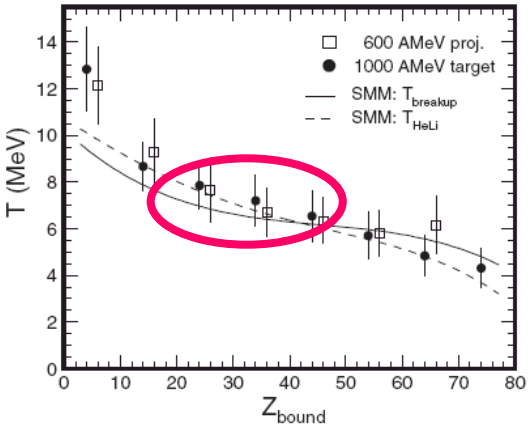

Au(600MeV/n)+C,Al,Cu

A.S.Botvina et al.,
Nucl.Phys. A584(1995)737

H.Xi et al.,
Z.Phys. A359(1997)397

comparison with SMM (statistical multifragmentation model)

Statistical equilibrium has been reached in these reactions

Au(600MeV/n)+Cu

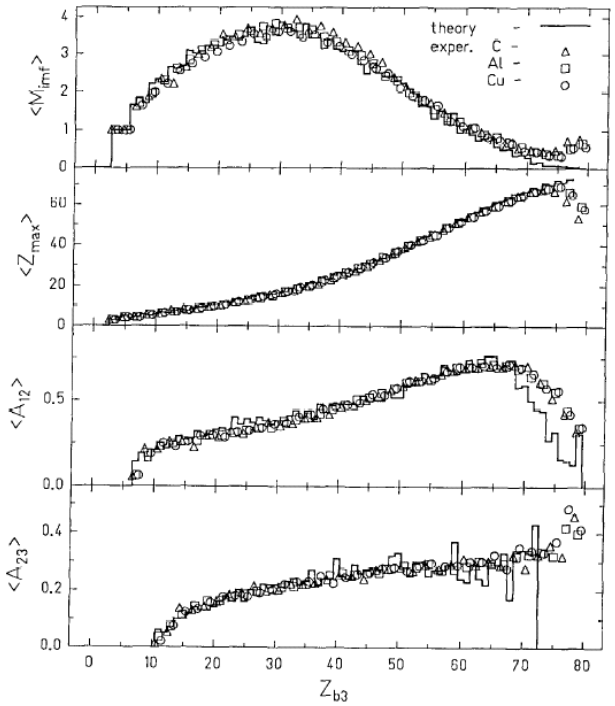

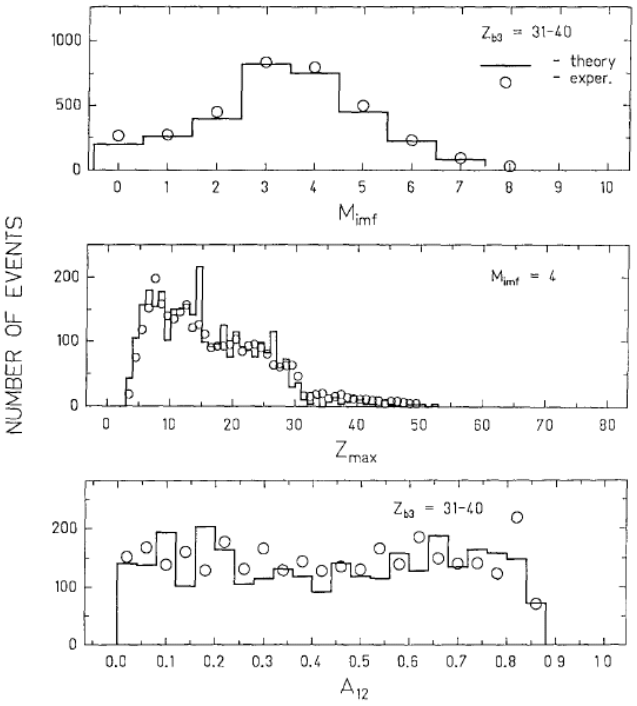

R.Ogul et al. PRC **83,** 024608 (2011) **ALADIN@GSI**

Isospin-dependent multifragmentation of relativistic projectiles

124,107-**Sn**, 124-**La** (600 A MeV) + **Sn** → projectile (multi-)fragmentation

Very good description is obtained within Statistical Multifragmentation Model, including fragment charge yields, isotope yileds, various fragment correlations.

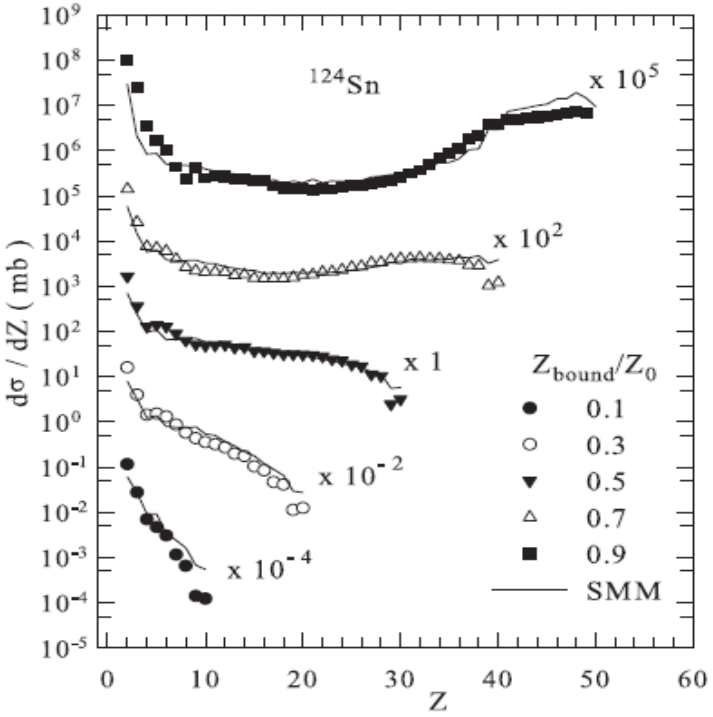

Statistical (chemical) equilibrium is established at break-up of hot projectile residues ! In the case of strangeness admixture we expect it too !

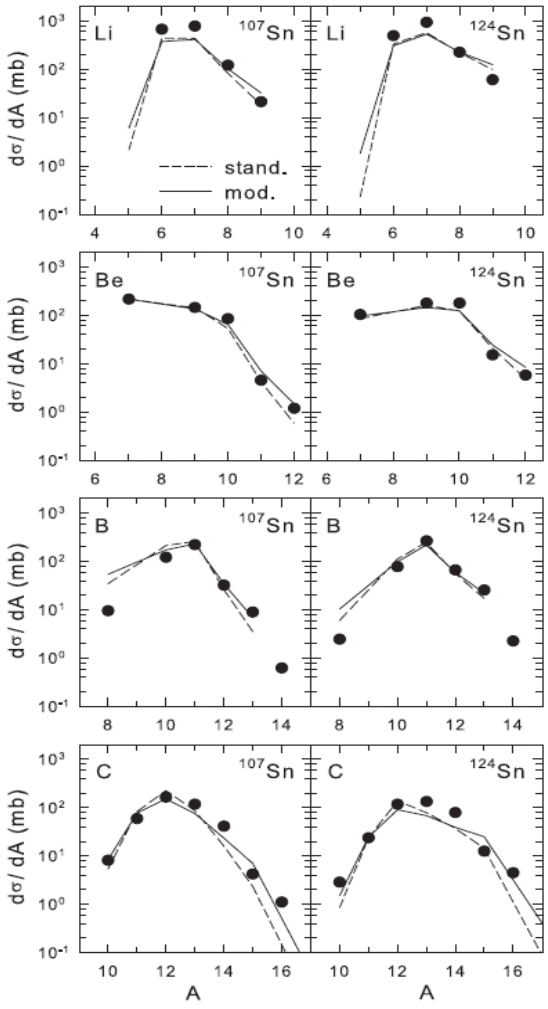

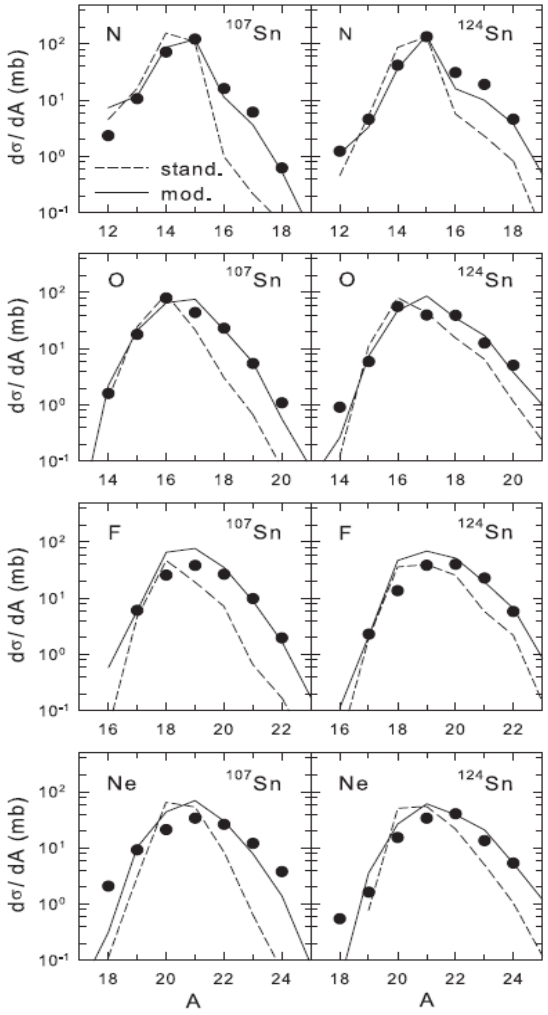

Production of excited hyper-residues in peripheral collisions, decaying into hypernuclei (target/projectile rapidity region).

DCM and UrQMD + CB predictions: Phys. Rev. C95, 014902 (2017)

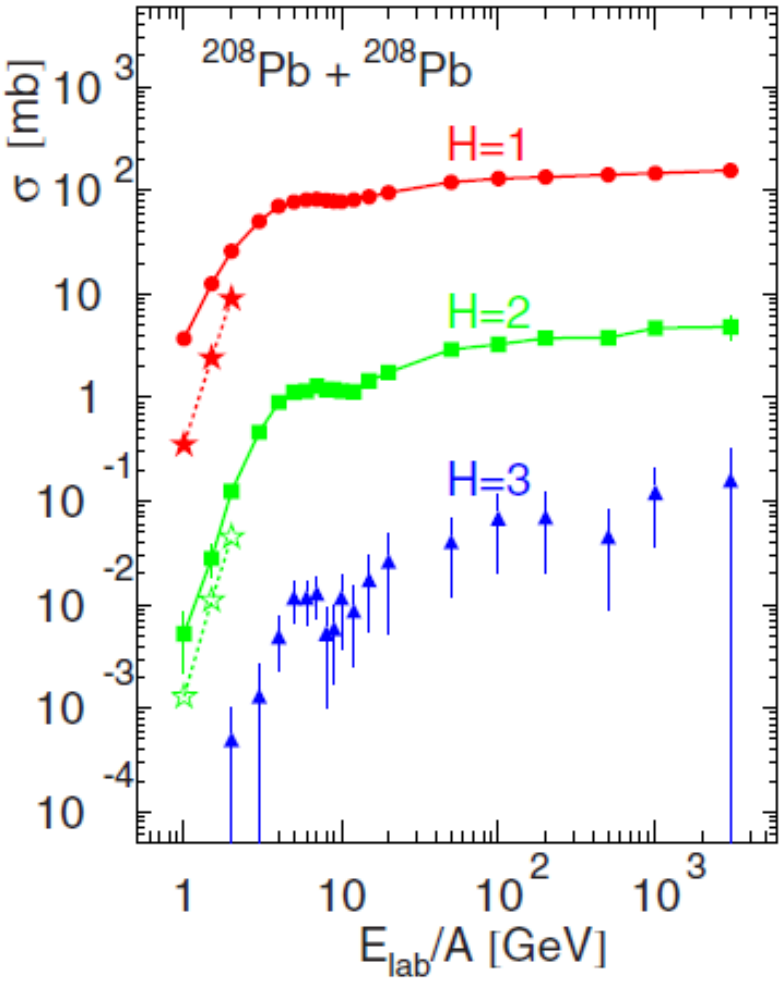

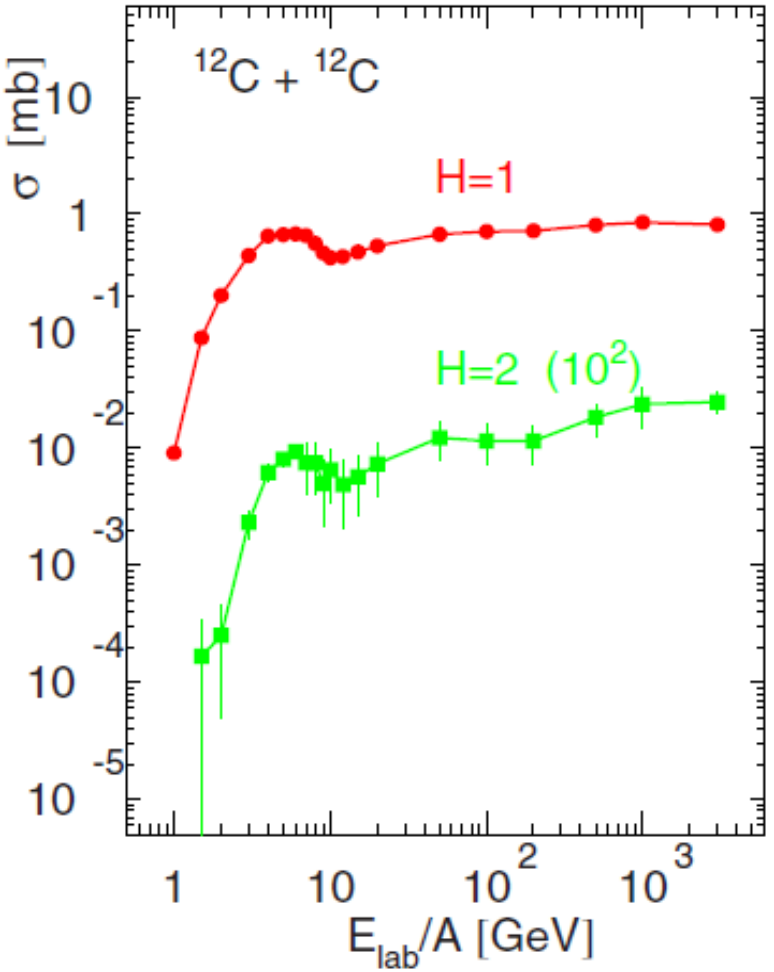

Production of light hypernuclei in relativistic ion collisions

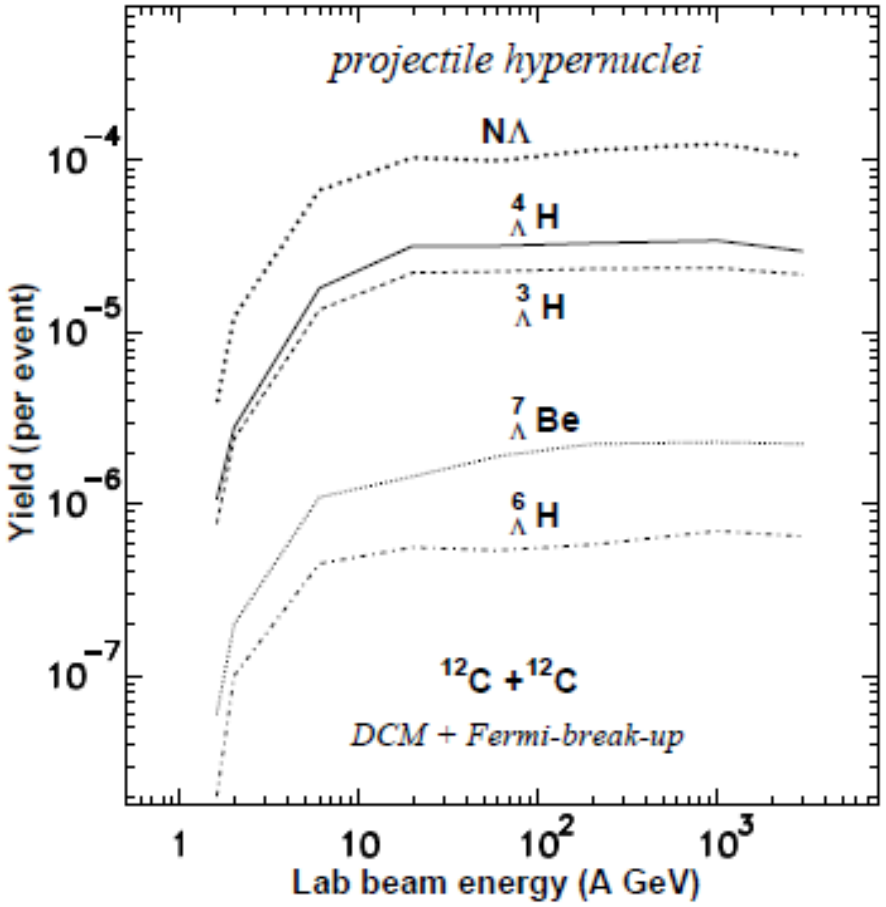

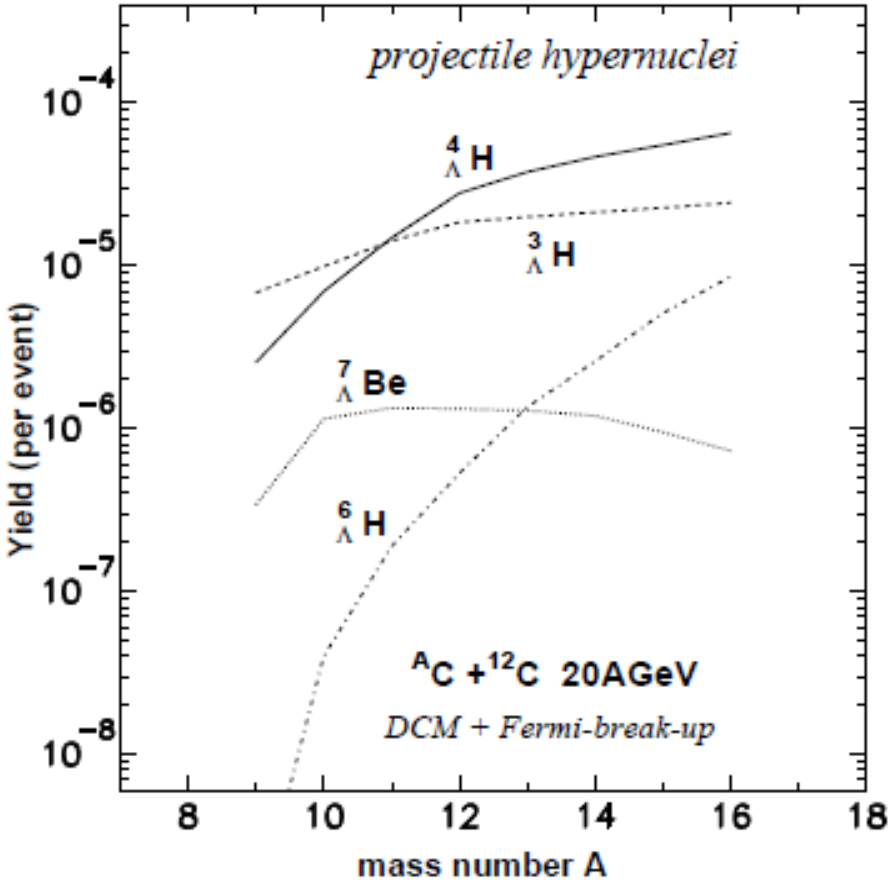

One can use exotic neutron-rich and neutron-poor projectiles, which are not possible to use as targets in traditional hyper-nuclear experiments, because of their short lifetime. Comparing yields of hypernuclei from various sources we can get info about their binding energies and properties of hyper-matter.

A.S.Botvina, K.K.Gudima, J.Pochodzalla, PRC 88, 054605, 2013

Statistical reaction models can be used not only for the production prediction:

Experimental yields of isotopes can be used for extracting properties of exotic cluster, e.g., the hyperon binding energies

Double ratio method :

ΔE_{bh} **vs** ΔA

difference of hyperon energies in hyper-nuclei:
Phys.Rev.C98(2018)064603

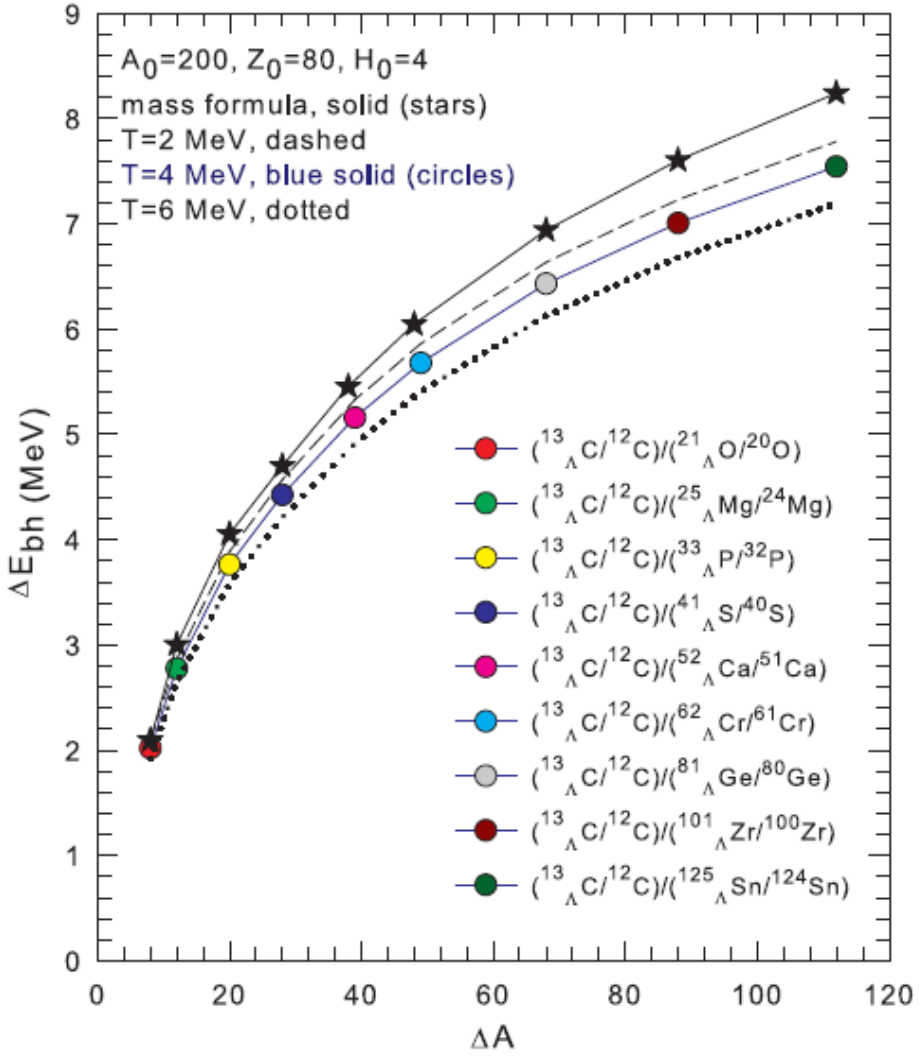

$$\Delta E_{bh} = T \cdot \left[ln\left(\frac{(g_{A_1,Z_1,H}/g_{A_1-1,Z_1,H-1}) \cdot (A_1^{3/2}/(A_1-1)^{3/2})}{(g_{A_2,Z_2,H}/g_{A_2-1,Z_2,H-1}) \cdot (A_2^{3/2}/(A_2-1)^{3/2})}\right) - ln\left(\frac{Y_{A_1,Z_1,H}/Y_{A_1-1,Z_1,H-1}}{Y_{A_2,Z_2,H}/Y_{A_2-1,Z_2,H-1}}\right)\right]$$

Formation of baryon clusters from the dynamically produced baryons as a results of secondary interaction between them, when they are in the vicinity of each other. Note: baryons in clusters can come to equilibrium and the clusters are excited respective to its ground state. This case is realized in Heavy- Ion collisions of medium/high energies.

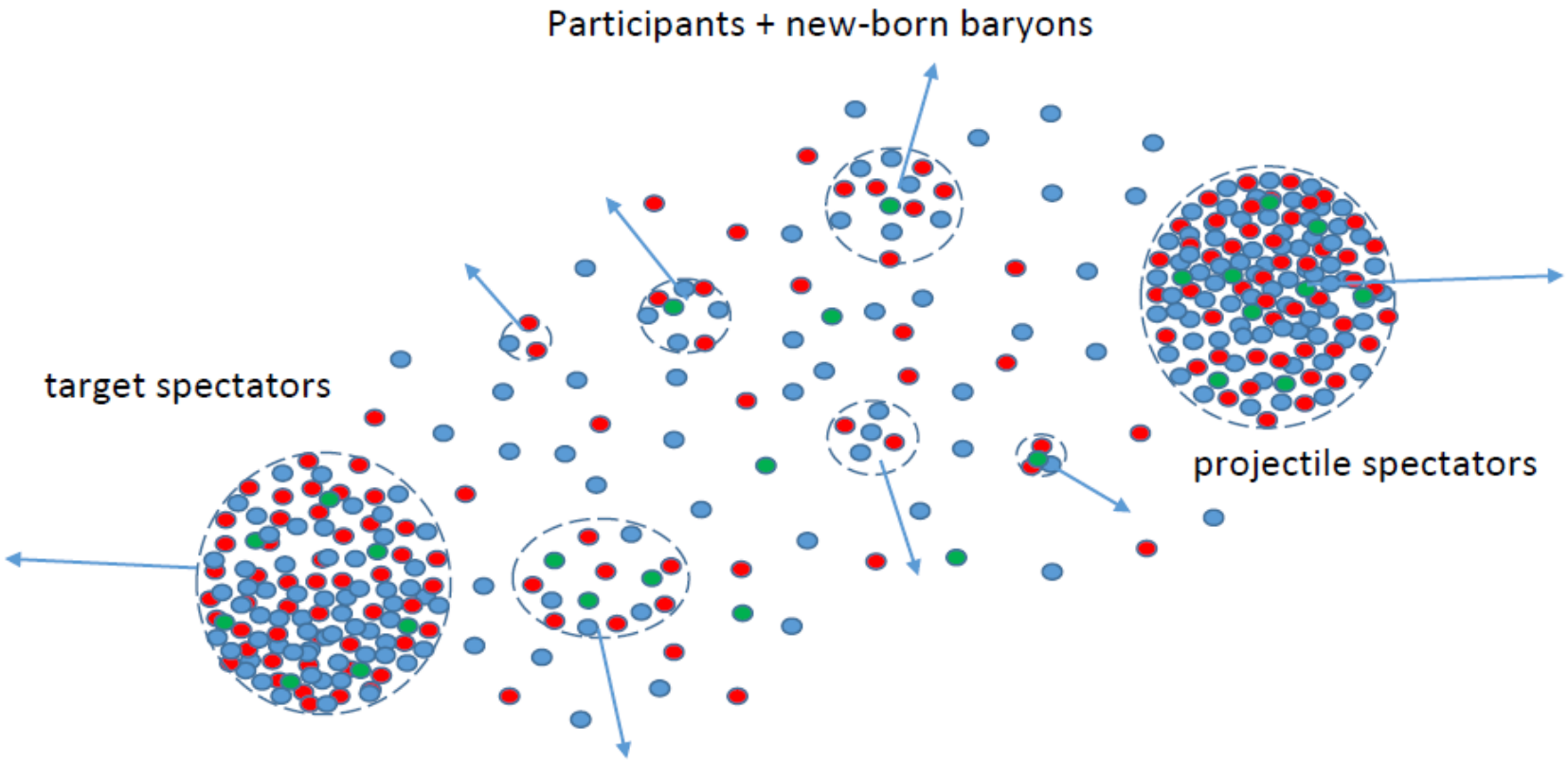

CENTRAL COLLISIONS

Nuclear system expands to low densities and passes the density around 0.1 of normal nuclear density, which corresponds to the freeze-out adopted in the statistical models. Baryons can still interact and form nuclei at this density. We divide the nuclear matter into clusters in local chemical equilibrium and apply SMM to describe the nucleation process in these clusters.

dynamical expansion after collision/compress.

Baryonic clusters in local equilibrium (freeze-out)

nuclei formation inside the clusters - SMM

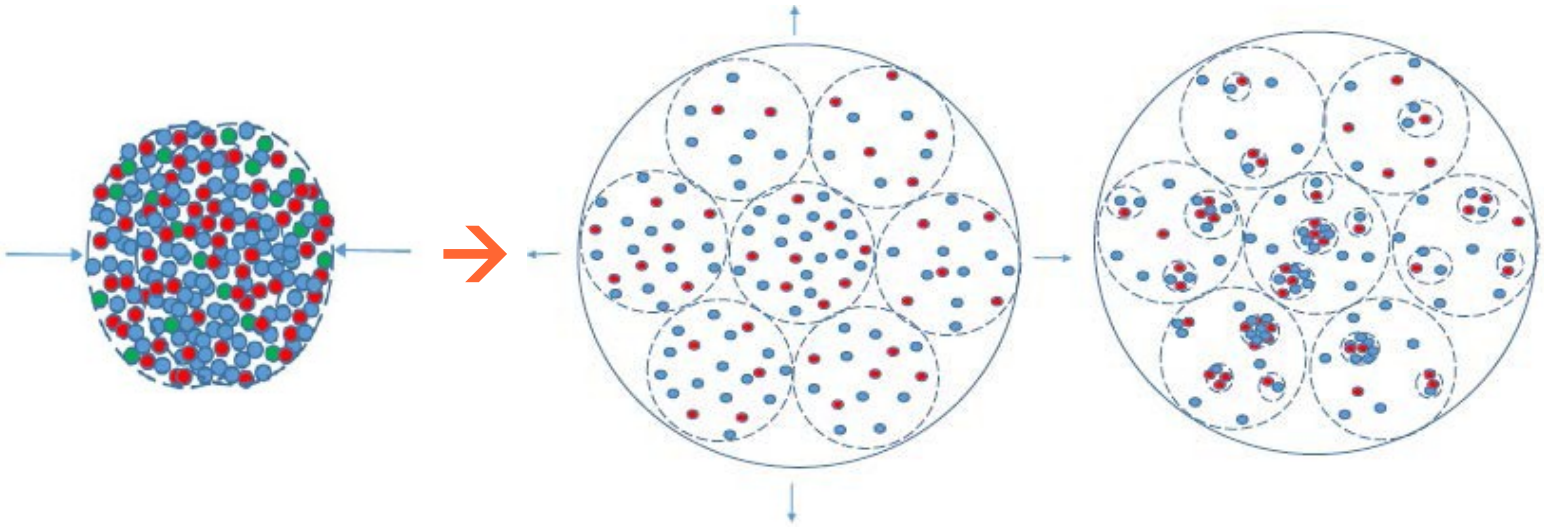

To check this novel mechanism with controlled models:

Phys.Rev.C103 (2021) 064602 and arXiv:2203.17092

The dynamical stage is simulated with the phase space generation (PSG) and hydrodynamical-like generation (HYG) methods. They provide very different momenta distributions of baryons which cover the most important limits expected after this stage.

Selection of primary clusters (at low freeze-out density) by using the coalescence of baryon (CB) model (Phys. Lett. B742, 7 (2015)): according to their velocities $|Vi - V0| \leq Vc$ **and coordinates** $|Xi - X0| \leq Xc$ **.**

Statistical formation of nuclei inside these clusters with SMM: de-excitation of the excited clusters. The excitation energy (or local temperature) of such clusters is important characteritics for the nuclear matter.

Nuclear system consists of primary clusters in local equilibrium:

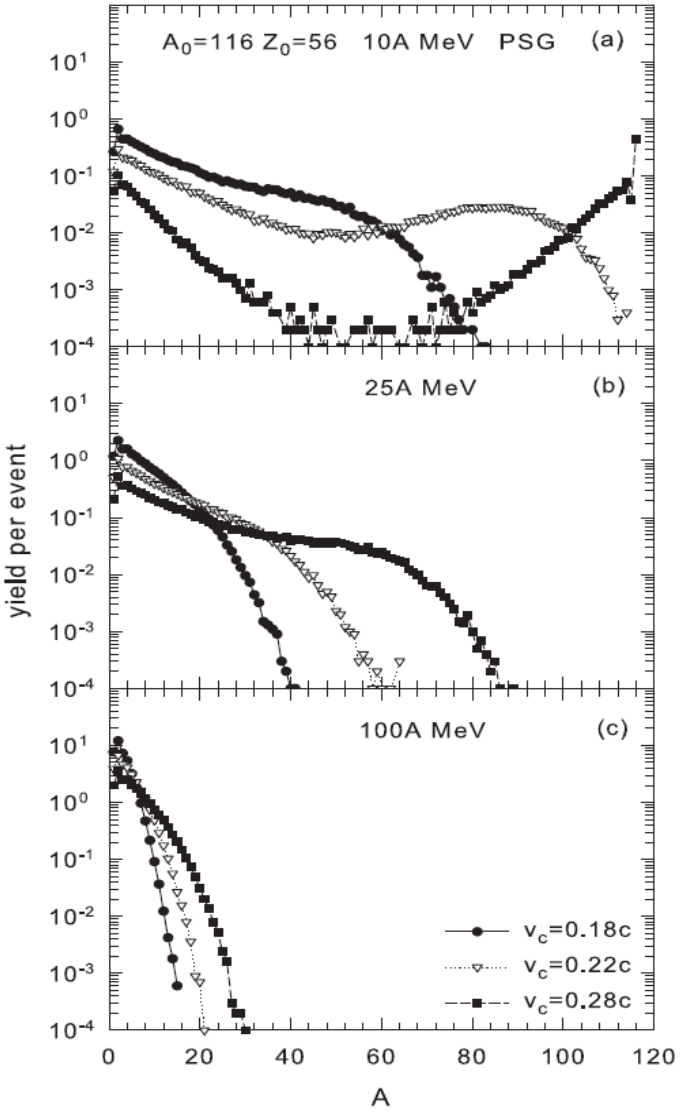

final nuclei after the statistical nucleation (disintegration of the excited clusters via SMM):

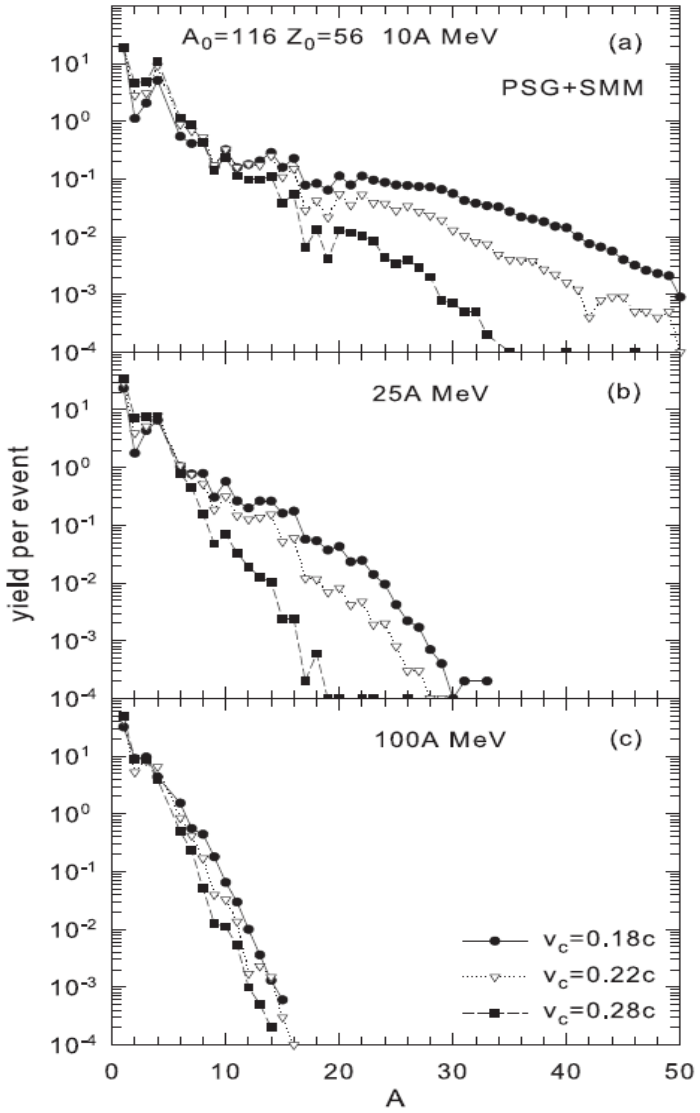

For the first, the consistent comparison with FOPI@GSI experimental data - Nucl. Phys. A848(2010)366 - on fragment production in central HI collisions is performed: Both charge yields and flow energies.
see Phys.Rev.C103 (2021) 064602 and arXiv:2203.17092

yields of nuclei in different reactions:

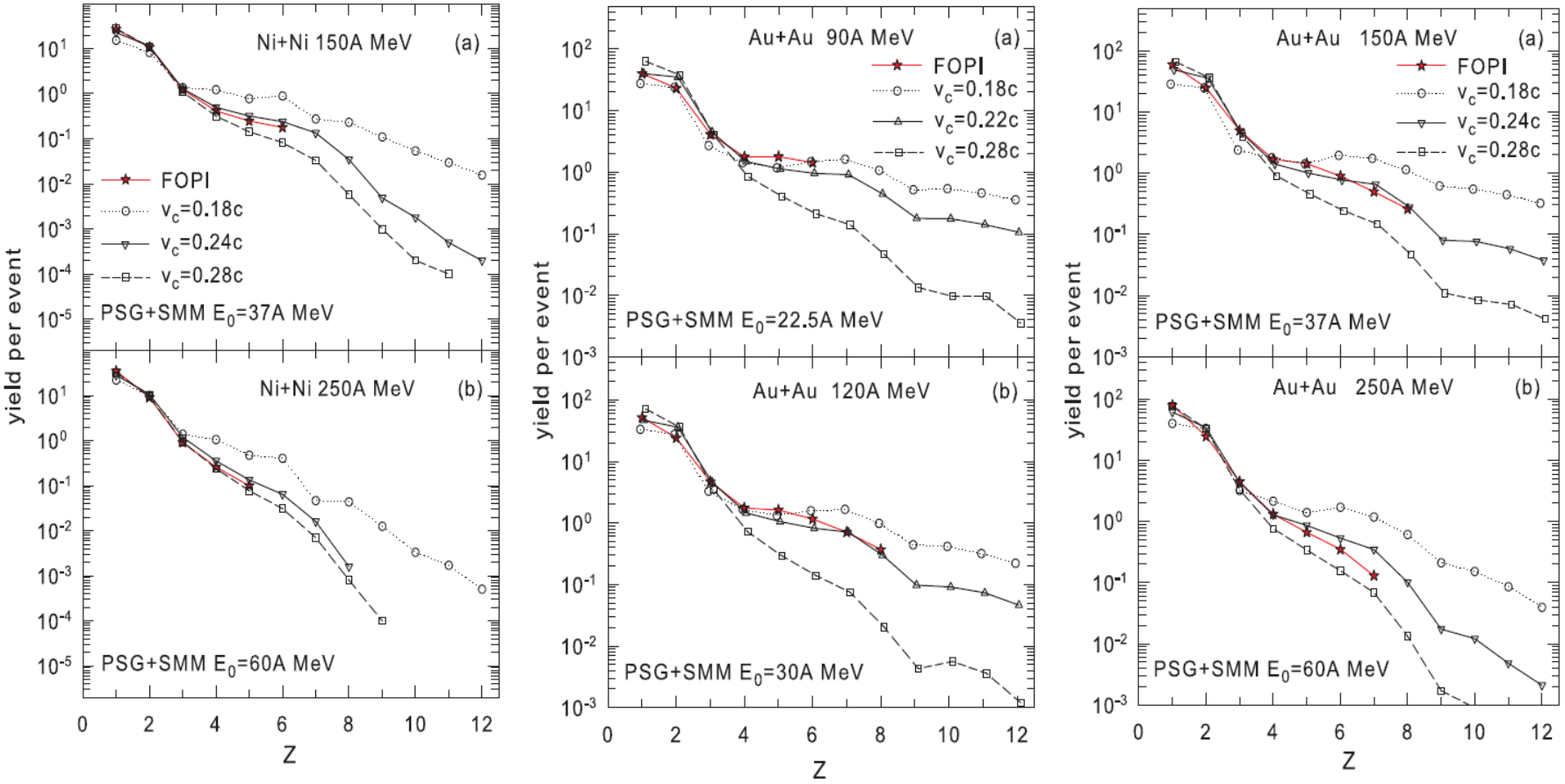

(until now the production of nuclei (Z>2) in central collisions was not possible to describe consistently)

kinetic energies of nuclei in different reactions:

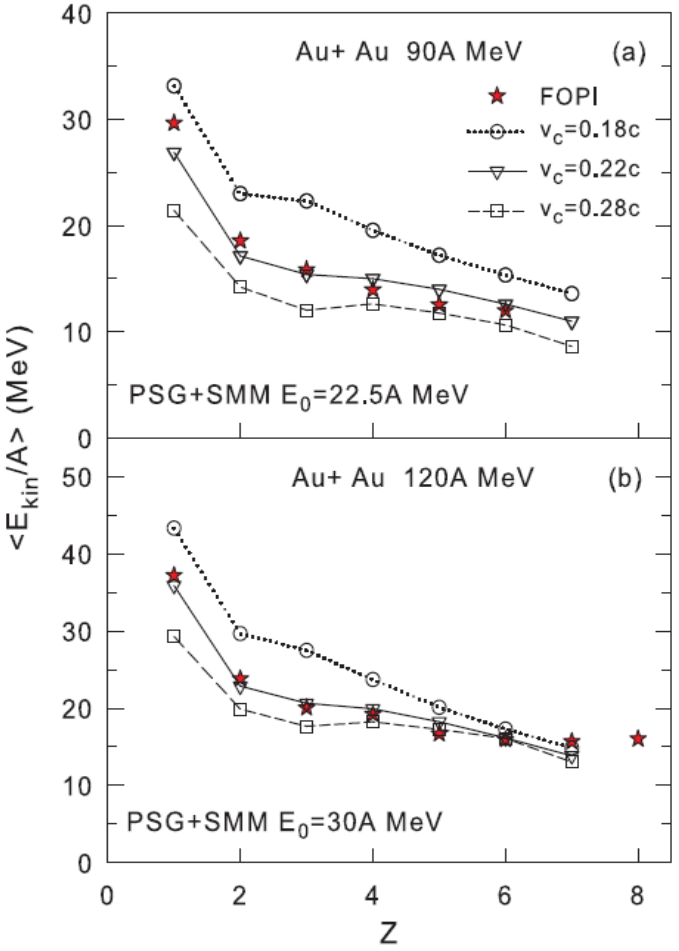

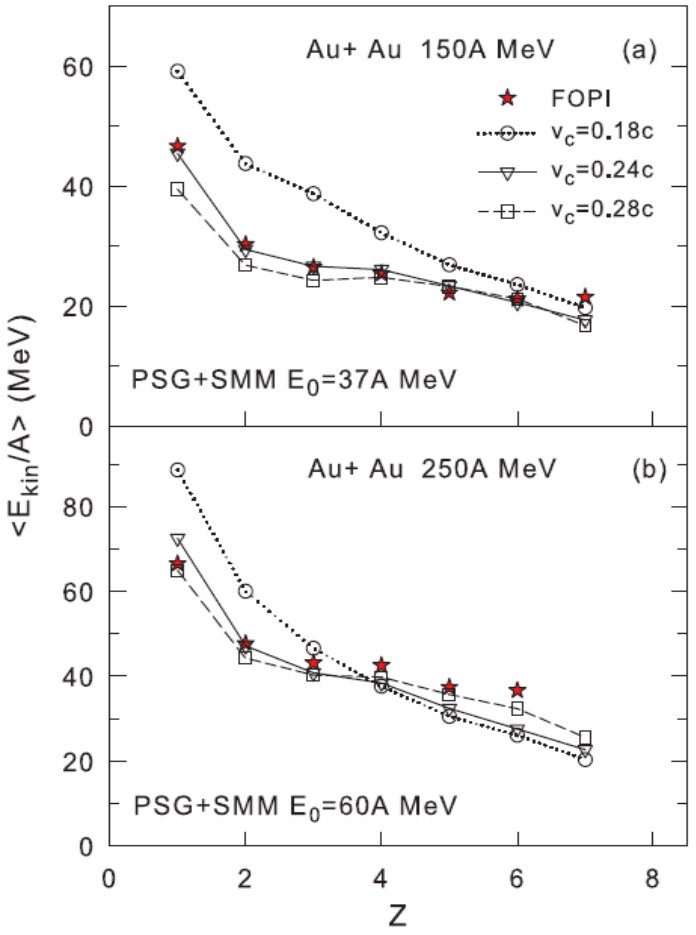

Important beam energy dependence of the light nuclei yields in Au+Au relativistic central collisions can be explained within our approach too.

Note: in simplistic coalescence picture yields of 3He are larger than 4He yields at all energies. FOPI experimental data (red symbols) show intersection with increasing energy.

Relative behavior of yields of 3He and 4He with energy is important confirmation of the nucleation via the statistical mechanism

Phys.Rev.C103 (2021) 064602

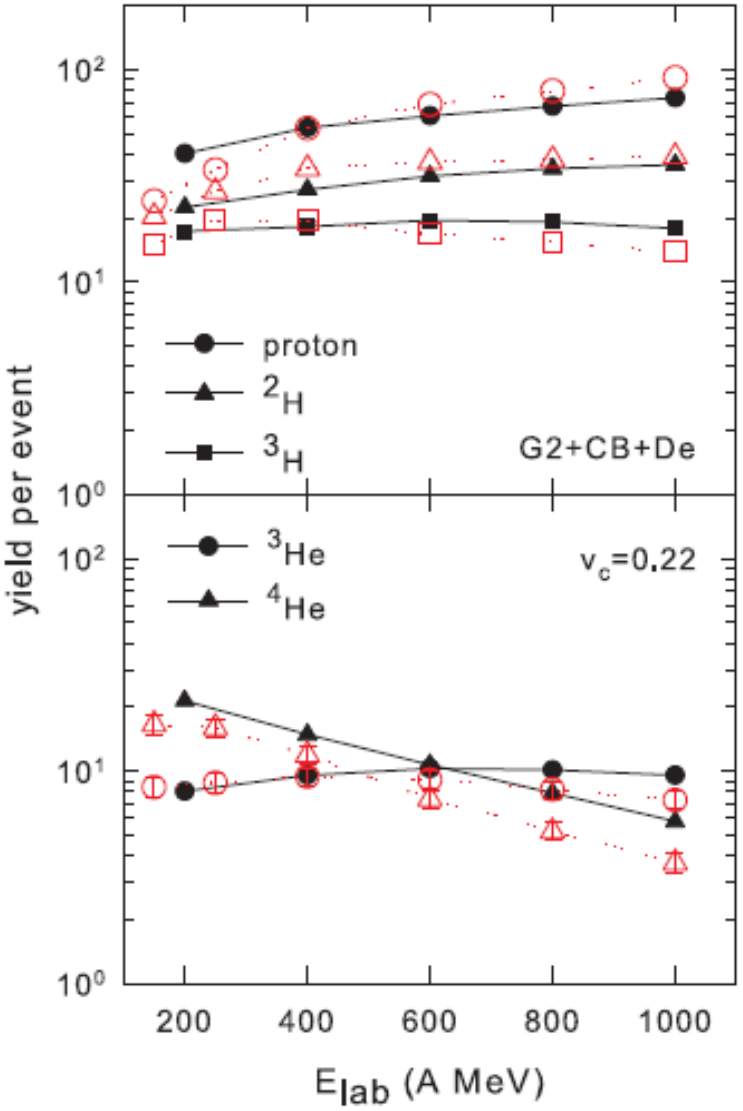

However, the description is possible if there is a limit for the excitation energy of the clusters: 6–10 MeV/nucleon, close to their binding energies. Temperature T=6--8 MeV (according to the statistical model) which corresponds to the coexistence region of the liquid-gas type phase transition in nuclear matter.

We may speak about an universal mechanism for nuclei formation both in peripheral and central heavy-ion collisions , independently on the way how the low density matter is produced: by thermal-like expansion of the excited residues (peripheral col.) or by dynamical-like expansion (central col.)

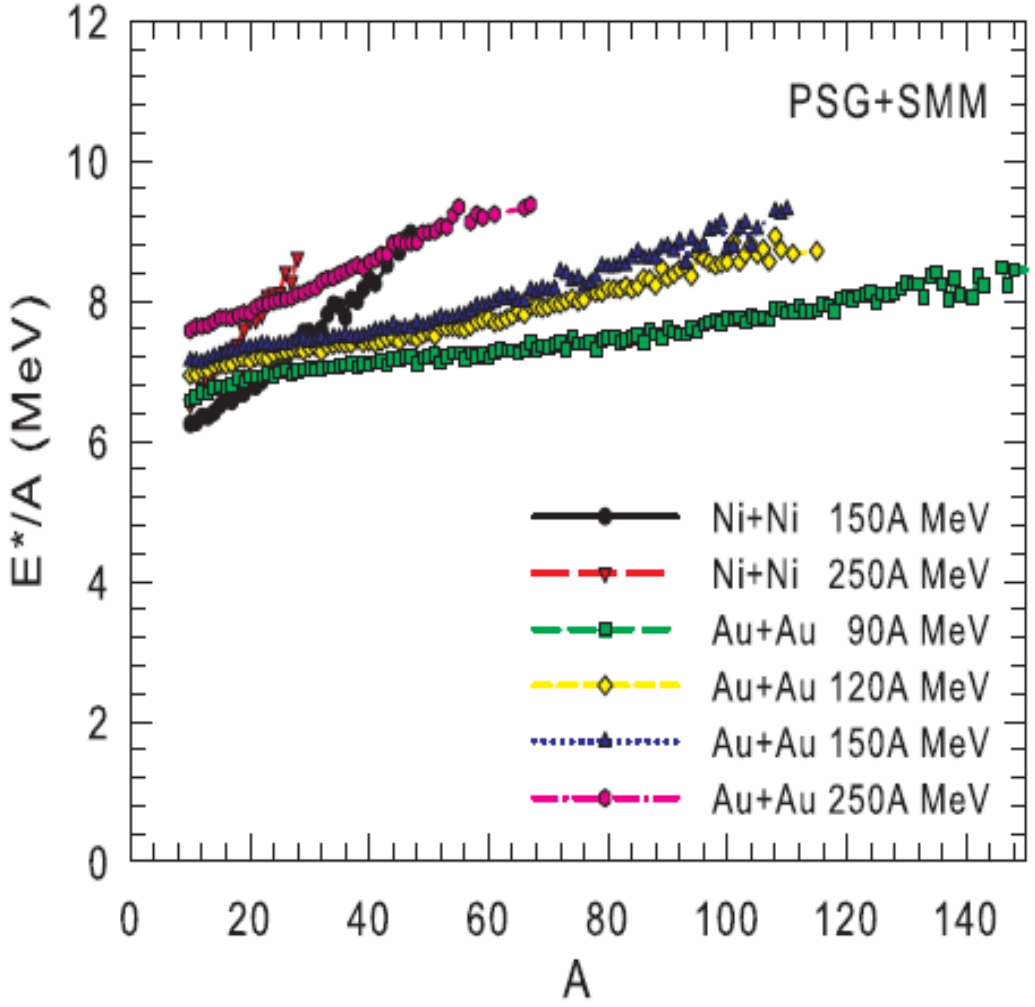

Theory conclusion on the energy dependence of nuclei production

Evolution of the statistical mechanism of the nucleation process in highly excited finite nuclear systems:

Compound nucleus conception –
excitation energies from 0 to 2-3 MeV/nucleon

Freeze-out volume conception –
excitation energies from 2-3 to 8-10 MeV/nucleon

At total energies more than 8-10 MeV/nucleon – fragmentation of the expanding nuclear matter at low density into locally equilibrated clusters with energies not higher than 8-10 MeV/nucleon and production of final nuclei after the decay of such clusters.

Production of hypernuclei in HI central collisions

Basing on this general mechanism we can predict the hypernuclei yields in relativistic central collisions too. Many different light hypernuclei can be produced. The correlations between nuclear species exist and it can be used for their identification.

Phys.Rev.C103 (2021) 064602

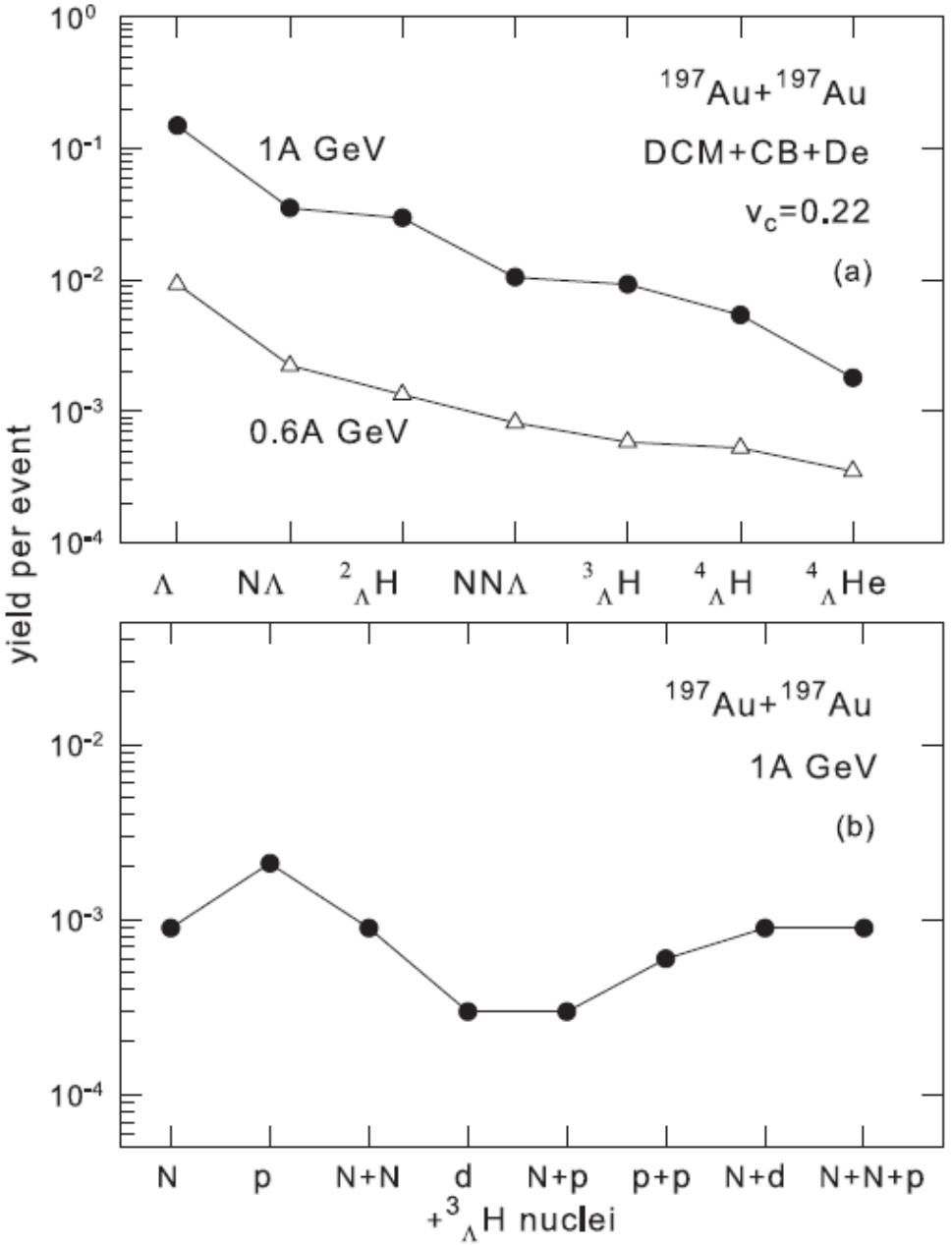

Conclusions

Collisions of relativistic ions are promising reactions to search for nuclear clusters, exotic clusters with very different isospin, including hypernuclei. These processes can be simulated within dynamical and statistical models.

Mechanisms of formation of hypernuclei in reactions: Strange baryons (Λ, Σ, Ξ, …) produced in particle collisions can be transported to the spectator residues and captured in nuclear matter. Another mechanism is the nucleation of baryons at subnuclear density. It leads to light clusters and is effective at all rapidities. Novel mechanism: The matter is divided into excited baryon clusters in local equilibrium and after the cluster decay the nuclei and hypernuclei of all sizes (and isospin), including short-lived weakly-bound states, multi-strange nuclei can be produced.

Advantages over other reactions: there is no limit on sizes and isotope content of produced exotic nuclei; probability of their formation may be high; a large strangeness can be deposited in nuclei.

Properties of hypernuclei (hyperon binding) can be addressed in novel way!

Correlations (unbound states) and lifetimes can be naturally studied.

EOS and the symmetry energy of hypermatter at subnuclear density and hyperon interactions in exotic nuclear matter can be investigated.

Excitation energies of the nuclear spectator residuals

DCM : PRC95, 014902 (2017)

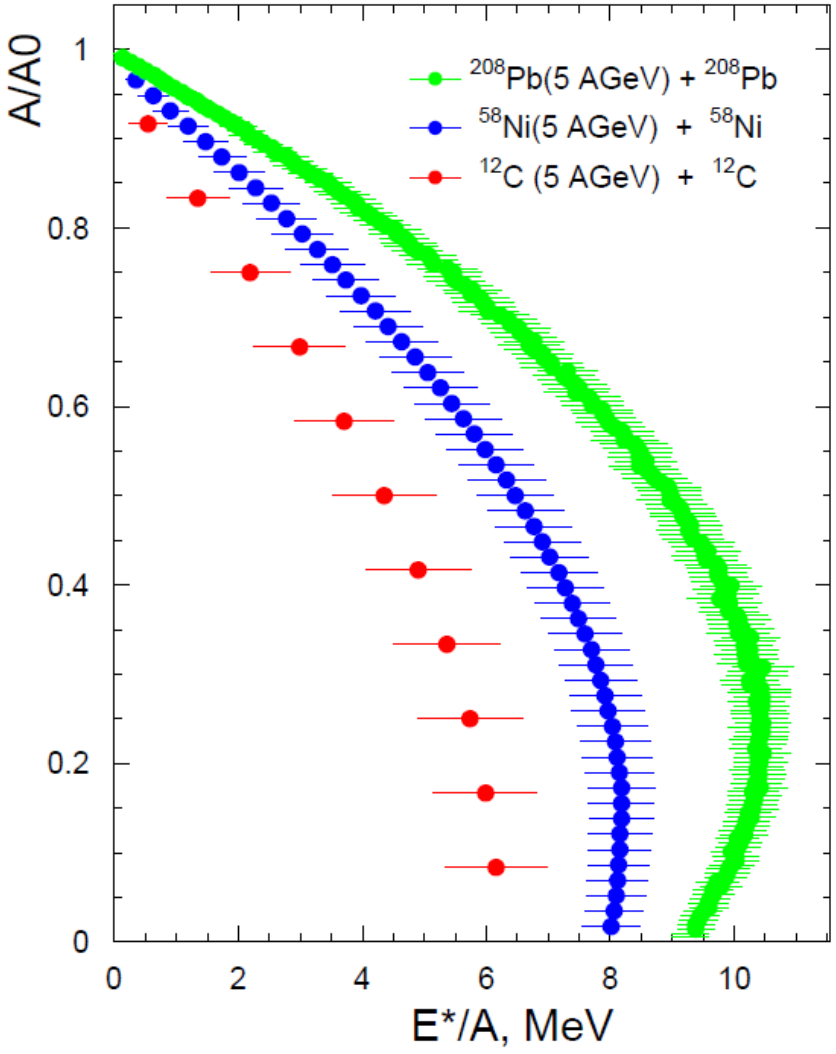

PRC84, 064904 (2011)

Masses of projectile residuals produced at dynamical stage (6b: H=0, 0.2b: H>0)

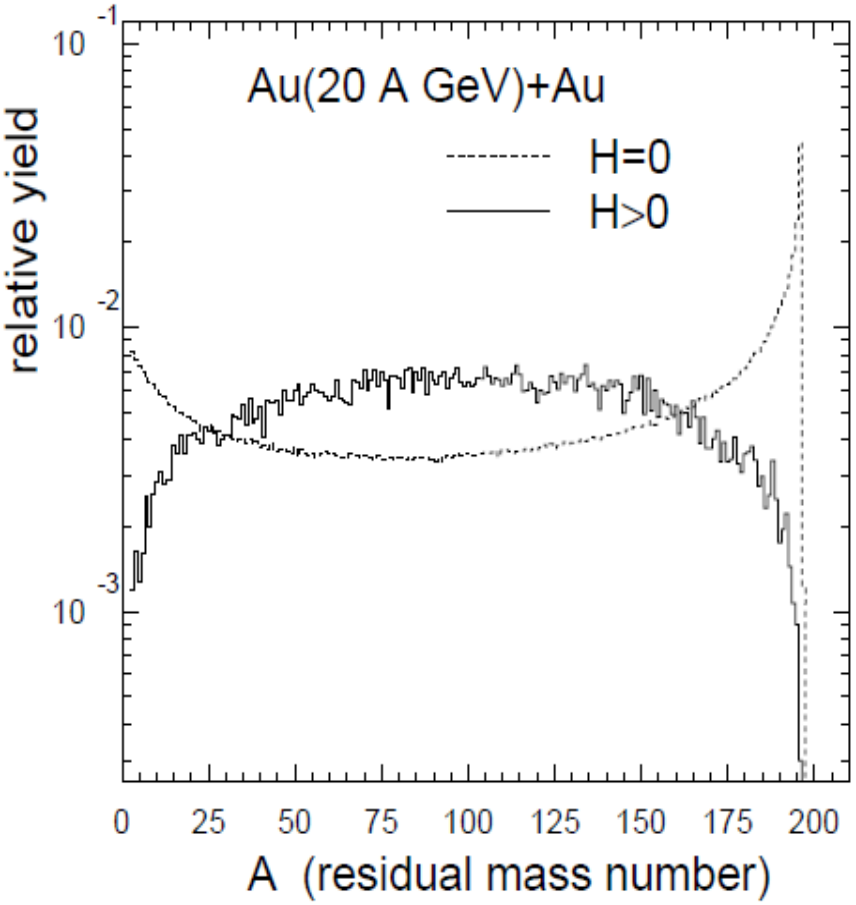

Discovery of a Strange nucleus: Hypernucleus

M. Danysz and J. Pniewski, Philos. Mag. 44 (1953) 348

First-hypernucleus was observed in a stack of photographic emulsions exposed to cosmic rays at about 26 km above the ground.

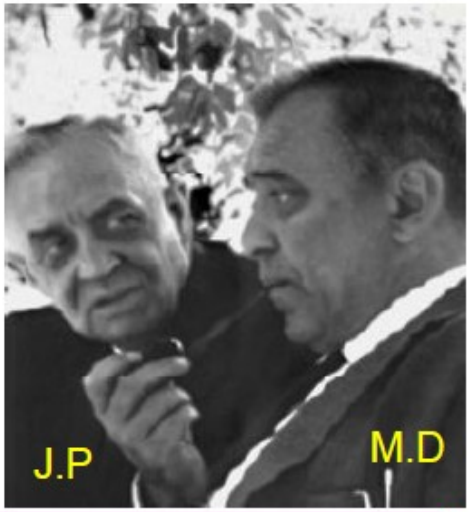

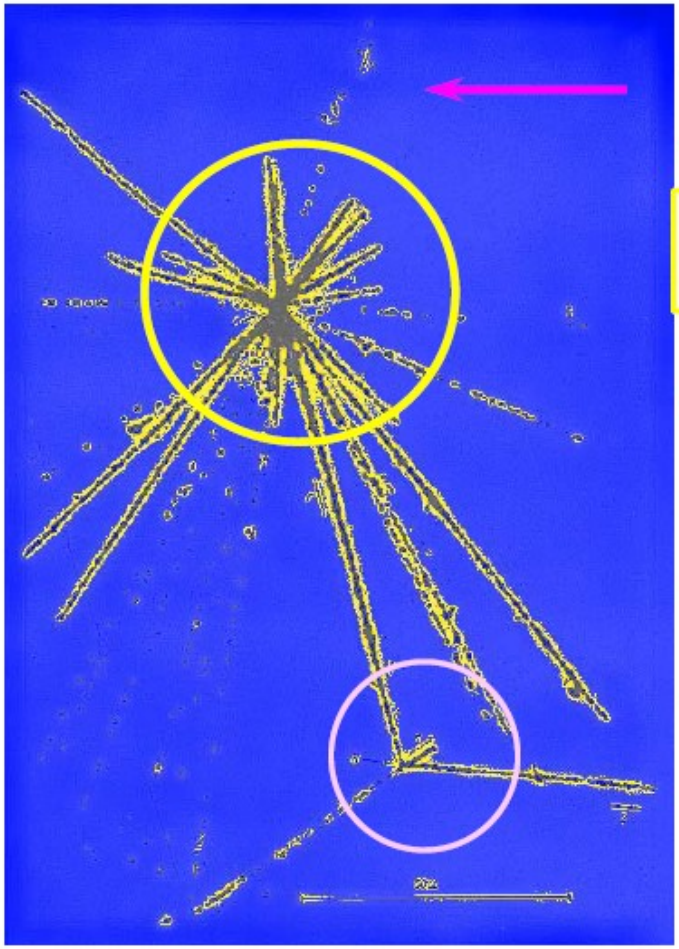

Incoming high energy proton from cosmic ray

colliding with a nucleus of the emulsion, breaks it in several fragments forming a star. **Multifragmentation !**

All nuclear fragments stop in the emulsion after a short path

From the first star, 21 Tracks => $9\alpha + 11H + 1\ {}_{\Lambda}X$

The fragment ${}_{\Lambda}X$ disintegrates later , makes the bottom star. Time taken ~ 10^{-12} sec (typical for weak decay)

This particular nuclear fragment, and the others obtained afterwards in similar conditions, were called **hyperfragments or hypernuclei.**

Dynamical+Statistical description of normal multifragmentation

ALADIN data

GSI

multifragmentation of relativistic projectiles

A.S.Botvina et al., Nucl.Phys. A584(1995)737

comparison with SMM (statistical multifragmentation model)

Statistical equilibrium has been reached in these reactions

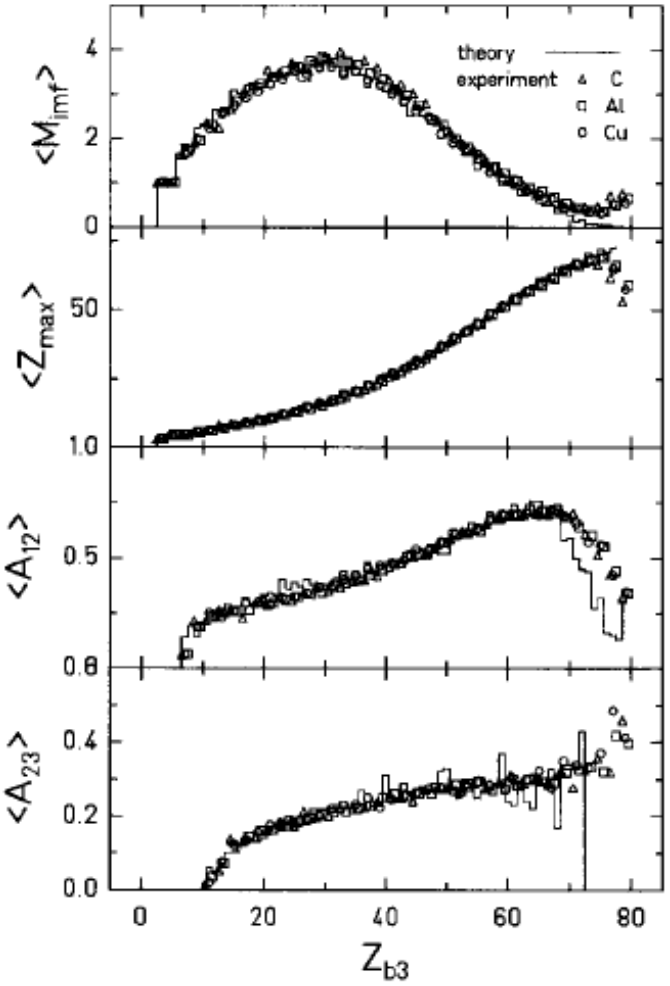

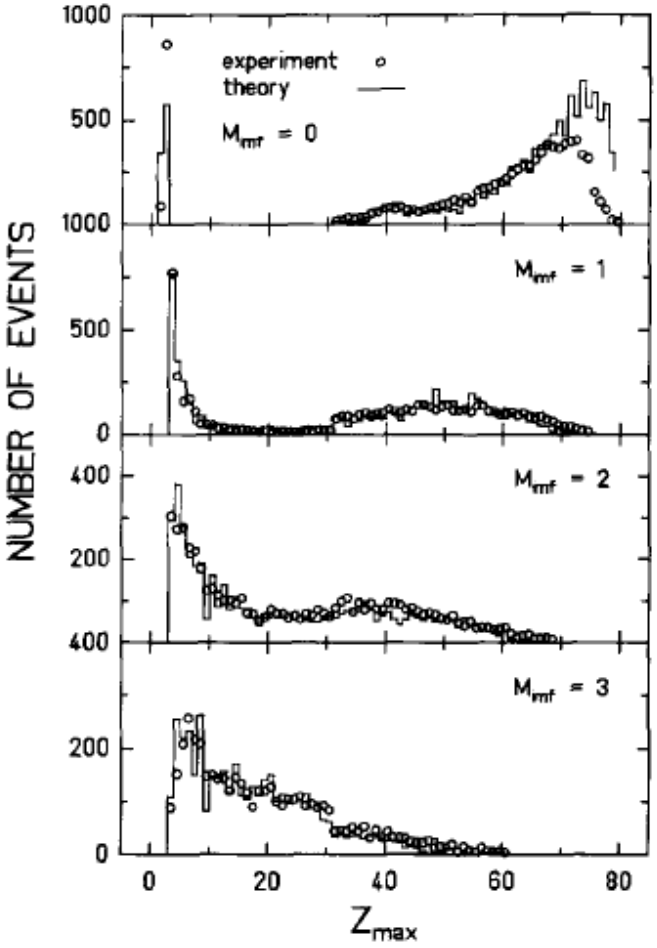

Correlation characteristics are very important for verification of models !

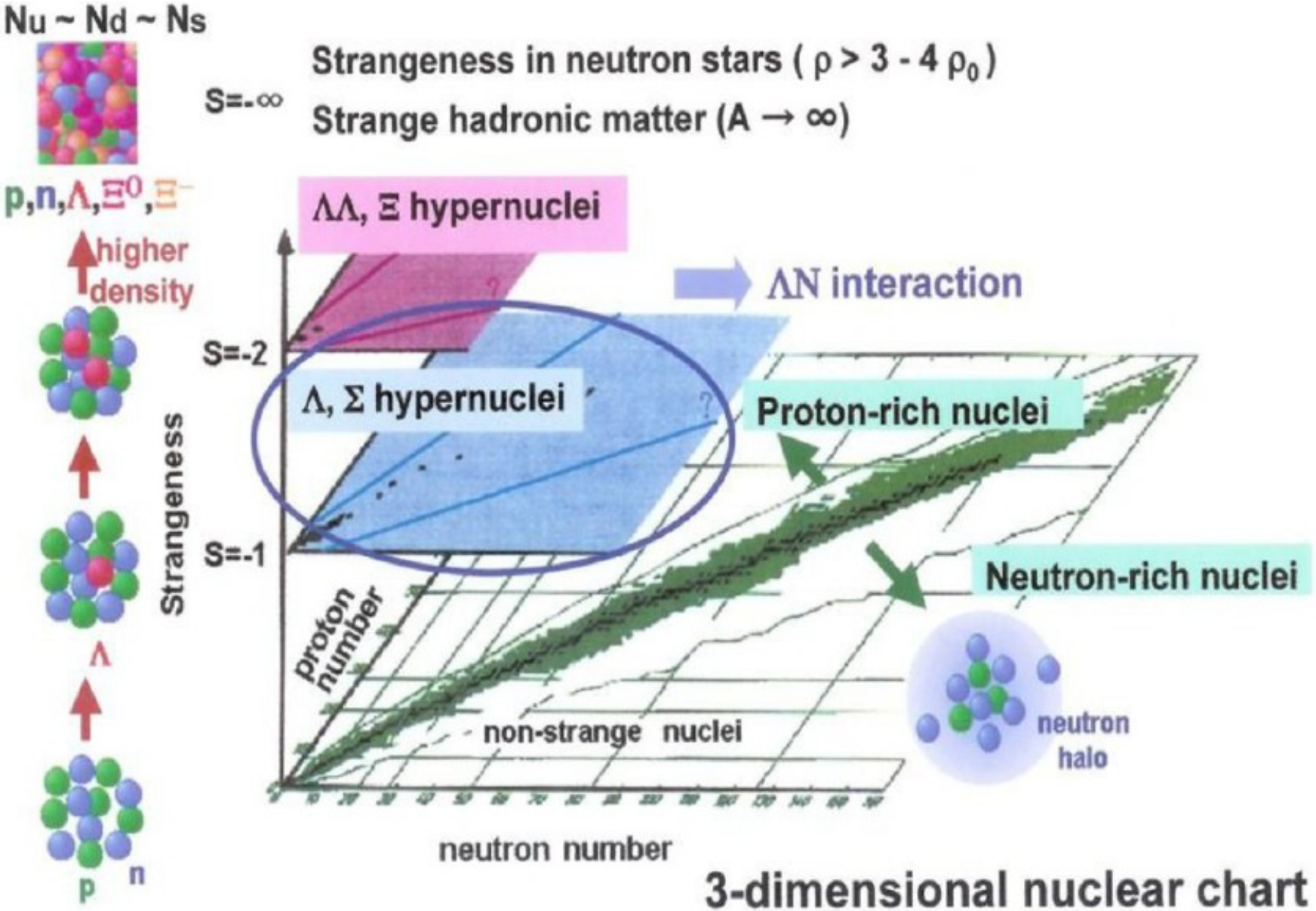
Nu ~ Nd ~ Ns
Strangeness in neutron stars (ρ > 3 - 4 ρ0)
S=-∞
Strange hadronic matter (A → ∞)
p,n,Λ,Ξ0,Ξ−
higher density
ΛΛ, Ξ hypernuclei
ΛN interaction
S=-2
Λ, Σ hypernuclei
Proton-rich nuclei
S=-1
Neutron-rich nuclei
Strangeness
proton number
non-strange nuclei
neutron halo
neutron number
Λ
p
n
3-dimensional nuclear chart

Λ-hyperon lifetime in very heavy hypernuclei produced in the p+U interaction

The recoil shadow method for the detection of fission fragments has been used to investigate delayed fission of very heavy Λ hypernuclei produced in the p-U interaction at the projectile energy of 1.5 GeV. From the measured distribution of delayed fission events in the shadow region and the calculated momenta of hypernuclei leaving the target the lifetime of the Λ hyperon in very heavy hypernuclei was determined to be $\tau = 2.40 \pm 60$ ps. The comparison of the number of delayed fission events with that of the prompt events leads to an estimation of the cross section for the production of Λ hypernuclei in p+U collisions at 1.5 GeV of $\sigma_{Hv} = 150^{+150}_{-80}$ μb. [S0556-2813(97)04506-8]

H. Ohm et al., PRC 55 (1997) 3062

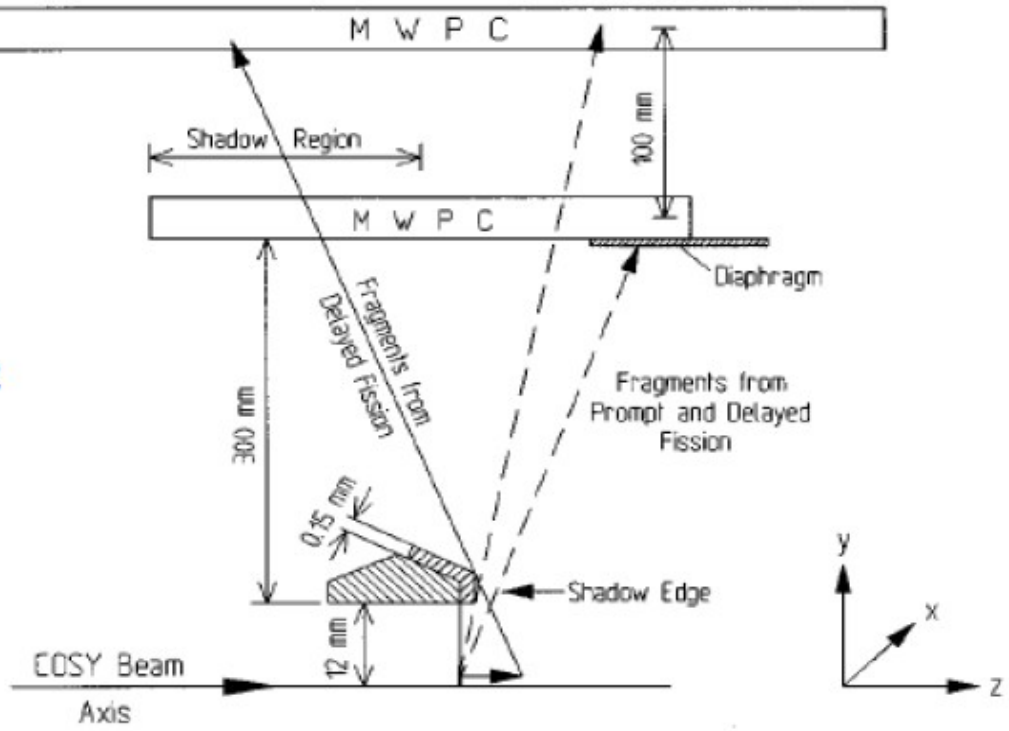

FIG. 1. Schematic presentation of the experimental setup. The thickness of the target holder is enhanced in the drawing to show the details. The real distances are given.

4.3.3. Evaporation from hot fragments

The successive particle emission from hot primary fragments with $A > 16$ is assumed to be their basic de-excitation mechanism. Due to the high excitation energy of these fragments, the standard Weisskopf evaporation scheme [2] was modified to take into account the heavier ejectiles up to ^{18}O, besides light particles (nucleons, d, t, α), in ground and particle-stable excited states [81]. This corresponds to the excitation energies $\epsilon^{(i)}$ of the ejectiles not higher than 7–8 MeV. By analogy with standard model the width for the emission of a particle j from the compound nucleus (A, Z) is given by:

$$\Gamma_j = \sum_{i=1}^{n} \int_0^{E^*_{AZ}-B_j-\epsilon_j^{(i)}} \frac{\mu_j g_j^{(i)}}{\pi^2 \hbar^3} \sigma_j(E) \frac{\rho_{A'Z'}(E^*_{AZ} - B_j - E)}{\rho_{AZ}(E^*_{AZ})} E\, dE \qquad (60)$$

Here the sum is taken over the ground and all particle-stable excited states $\epsilon_j^{(i)} (i = 0, 1, \ldots, n)$ of the fragment j, $g_j^{(i)} = (2s_j^{(i)} + 1)$ is the spin degeneracy factor of the ith excited state, μ_j and B_j are corresponding reduced mass and separation energy, E^*_{AZ} is the excitation energy of the initial nucleus (55), E is the kinetic energy of an emitted particle in the centre-of-mass frame. In Eq. (60) ρ_{AZ} and $\rho_{A'Z'}$ are the level densities of the initial (A, Z) and final (A', Z') compound nuclei. They are calculated using the Fermi-gas formula (41). The cross section $\sigma_j(E)$ of the inverse reaction $(A', Z') + j = (A, Z)$ was calculated using the optical model with nucleus–nucleus potential from Ref. [117]. The evaporational process was simulated by the Monte Carlo method using the algorithm described in Ref. [118]. The conservation of energy and momentum was strictly controlled in each emission step.

Evaporation from hypernuclei: nucleons, light particles, hyperons, light hypernuclei: New masses and assuming the level densities as in normal nuclei.

4.3.4. Nuclear fission

An important channel of de-excitation of heavy nuclei ($A > 200$) is fission. This process competes with particle emission. Following the Bohr–Wheeler statistical approach we assume that the partial width for the compound nucleus fission is proportional to the level density at the saddle point $\rho_{sp}(E)$ [1]:

$$\Gamma_f = \frac{1}{2\pi\rho_{AZ}(E^*_{AZ})} \int_0^{E^*_{AZ}-B_f} \rho_{sp}(E^*_{AZ} - B_f - E)\, dE, \tag{61}$$

where B_f is the height of the fission barrier which is determined by the Myers–Swiatecki prescription [120]. For approximation of ρ_{sp} we used the results of the extensive analysis of nuclear fissility and Γ_n/Γ_f branching ratios [121]. The influence of the shell structure on the level densities ρ_{sp} and ρ_{AZ} is disregarded since in the case of multifragmentation we are dealing with very high excitation energies $E^* > 30$–50 MeV when shell effects are expected to be washed out [122].

Fission of hypernuclei: New fission barriers including hyperon interaction (in the liquid-drop approach). It leads to increasing the barriers for ~ 1 MeV.
The level densities at the saddle point are taken as in normal nuclei (first approximation).

Evaporation & Fission of hypernuclei

(depending on mass and excitation energy)

A.S.Botvina et al., Phys. Rev. C94 (2016) 054615

These processes recall normal fission and evaporation. However, producing exotic hyper-fragments is possible (e.g. neutron rich ones) to investigate hyperon interactions in astro-physical conditions.

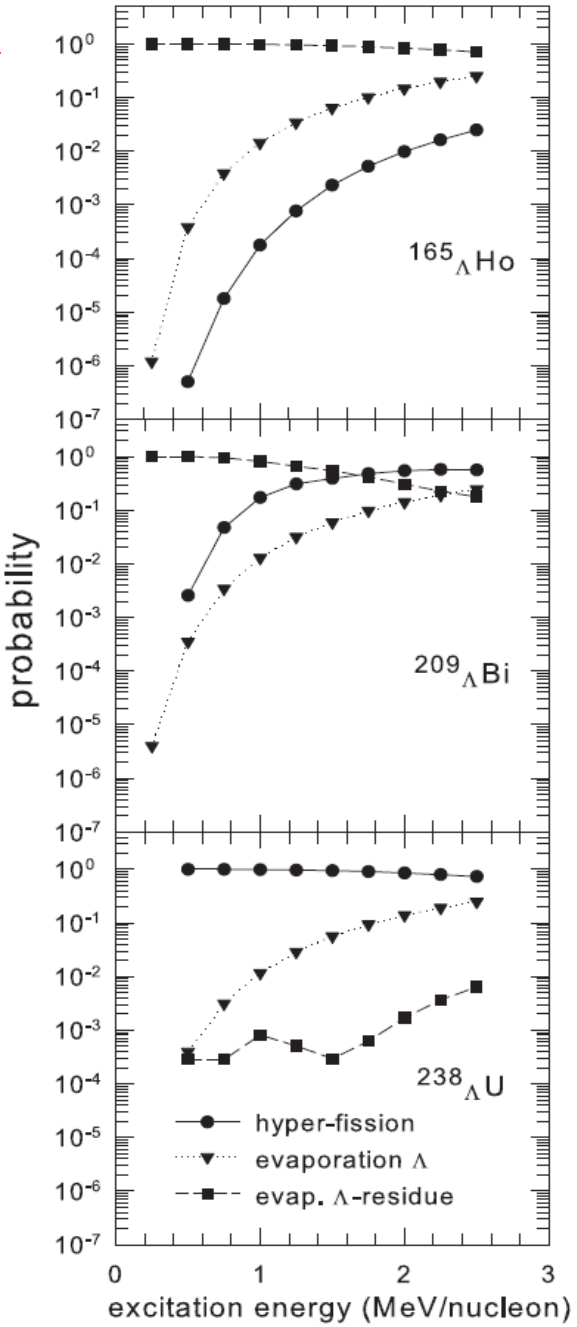

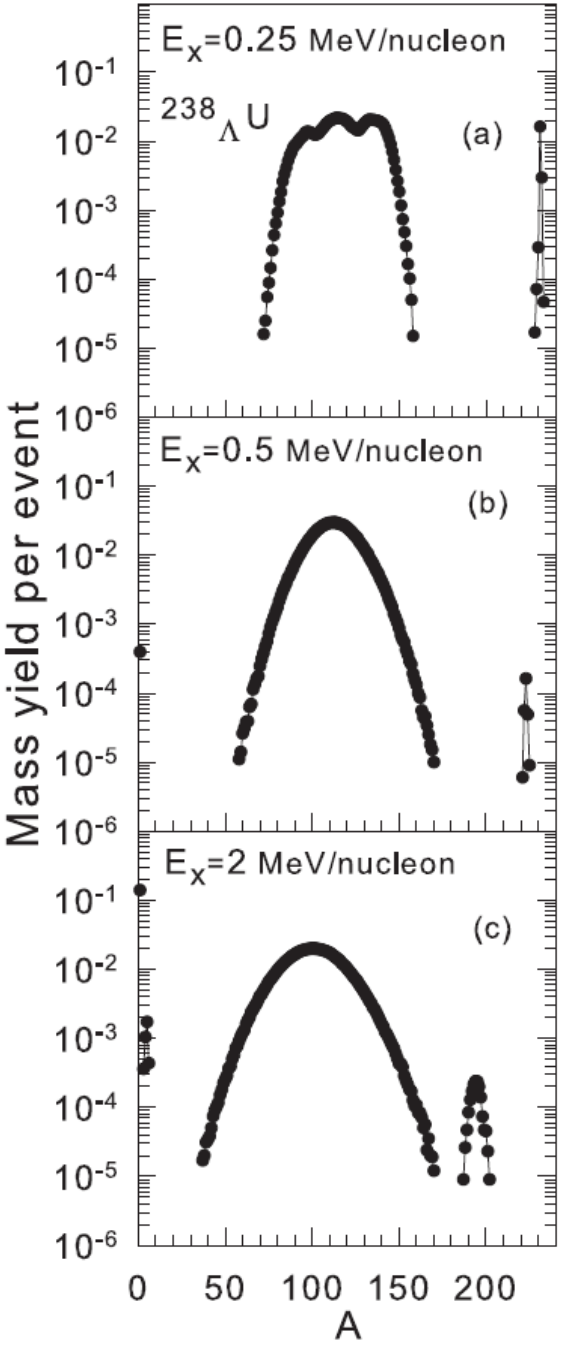

T.Saito, (for HypHI),
NUFRA2011 conference, and
Nucl. Phys. A881 (2012) 218;
Nucl. Phys. A913 (2013) 170.

C. Rappold et al.,
Phys. Rev. C88 (2013) 041001:
Λnn bound state ?

Production of hypernuclei in peripheral HI collisions: The HypHI project at GSI

T.R. Saito[a,b,c], D. Nakajima[a,d], C. Rappold[a,c,e], S. Bianchin[a], O. Borodina[a,b], V. Bozkurt[a,f], B. Göküzüm[a,f], M. Kavatsyuk[g], E. Kim[a,h], Y. Ma[a,b], F. Maas[a,b,c], S. Minami[a], B. Özel-Tashenov[a], P. Achenbach[b], S. Ajimura[i], T. Aumann[a], C. Ayerbe Gayoso[b], H.C. Bhang[f], C. Caesar[a], S. Erturk[f], T. Fukuda[j], E. Guliev[h], Y. Hayashi[k], T. Hiraiwa[k], J. Hoffmann[a], G. Ickert[a], Z.S. Ketenci[f], D. Khaneft[a,b], M. Kim[h], S. Kim[h], K. Koch[a], N. Kurz[a], A. Le Fevre[a,l], Y. Mizoi[j], M. Moritsu[k], T. Nagae[k], L. Nungesser[b], A. Okamura[k], W. Ott[a], J. Pochodzalla[b], A. Sakaguchi[m], M. Sako[k], C.J. Schmidt[a], M. Sekimoto[n], H. Simon[a], H. Sugimura[k], T. Takahashi[n], G.J. Tambave[g], H. Tamura[o], W. Trautmann[a], S. Voltz[a], N. Yokota[k], C.J. Yoon[h], K. Yoshida[m],

Projectile fragmentation: ^{6}Li beam at 2 A GeV on ^{12}C target

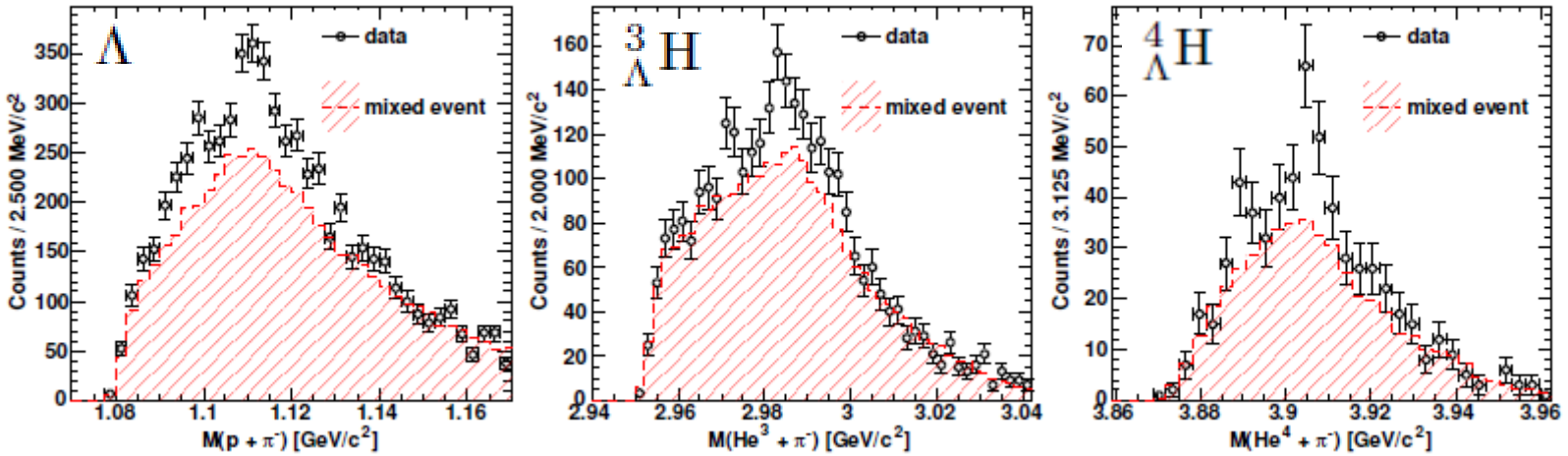

They have also observed a large correlation of $^{2}\mathrm{H} + \pi^{-}$
i.e., may be considerable production of Λn states

De-excitation of hot light hypernuclear systems

A.Sanchez-Lorente, A.S.Botvina, J.Pochodzalla, Phys. Lett. B697 (2011)222

For light primary fragments (with $A \leq 16$) even a relatively small excitation energy may be comparable with their total binding energy. In this case we assume that the principal mechanism of de-excitation is the explosive decay of the excited nucleus into several smaller clusters (the secondary break-up). To describe this process we use the famous Fermi model [105]. It is analogous to the above-described statistical model, but all final-state fragments are assumed to be in their ground or low excited states. In this case the statistical weight of the channel containing n particles with masses m_i $(i = 1, \ldots, n)$ in volume V_f may be calculated in microcanonical approximation:

$$\Delta\Gamma_f^{\mathrm{mic}} \propto \frac{S}{G}\left(\frac{V_f}{(2\pi\hbar)^3}\right)^{n-1}\left(\frac{\prod_{i=1}^{n} m_i}{m_0}\right)^{3/2}\frac{(2\pi)^{(3/2)(n-1)}}{\Gamma(\frac{3}{2}(n-1))}\left(E_{\mathrm{kin}} - U_f^C\right)^{(3/2)n-5/2}, \qquad (58)$$

where $m_0 = \sum_{i=1}^{n} m_i$ is the mass of the decaying nucleus, $S = \prod_{i=1}^{n}(2s_i + 1)$ is the spin degeneracy factor (s_i is the ith particle spin), $G = \prod_{j=1}^{k} n_j!$ is the particle identity factor (n_j is the number of particles of kind j). E_{kin} is the total kinetic energy of particles at infinity which is related to the prefragment excitation energy E^*_{AZ} as

$$E_{\mathrm{kin}} = E^*_{AZ} + m_0c^2 - \sum_{i=1}^{n} m_ic^2. \qquad (59)$$

U_f^C is the Coulomb interaction energy between cold secondary fragments given by Eq. (49), U_f^C and V_f are attributed now to the secondary break-up configuration.

Generalization of the Fermi-break-up model: new decay channels with hypernuclei were included ; masses and spins of hypernuclei and their excited states were taken from available experimental data and theoretical calculations

Statistical approach for fragmentation of hyper-matter

$$Y_{AZH} = g_{AZH} V_f \frac{A^{3/2}}{\lambda_T^3} \exp\left[-\frac{1}{T}\left(F_{AZH} - \mu_{AZH}\right)\right]$$

$$\mu_{AZH} = A\mu + Z\nu + H\xi$$

mean yield of fragments with mass number A, charge Z, and Λ-hyperon number H

$$F_{AZH}(T,V) = F_A^B + F_A^S + F_{AZH}^{sym} + F_{AZ}^C + F_{AH}^{hyp}$$

liquid-drop description of fragments: bulk, surface, symmetry, Coulomb (as in Wigner-Seitz approximation), and hyper energy contributions
J.Bondorf et al., Phys. Rep. **257** (1995) 133

$$F_A^B(T) = \left(-w_0 - \frac{T^2}{\varepsilon_0}\right) A \quad ,$$

$$F_A^S(T) = \beta_0 \left(\frac{T_c^2 - T^2}{T_c^2 + T^2}\right)^{5/4} A^{2/3} \quad ,$$

parameters ≈ Bethe-Weizsäcker formula:

$w_0 = 16$ MeV, $\beta_0 = 18$ MeV, $T_c = 18$ MeV

$$F_{AZH}^{sym} = \gamma \frac{(A - H - 2Z)^2}{A - H} \quad ,$$

$\gamma = 25$ MeV $\varepsilon_0 \approx 16$ MeV

$$\sum_{AZH} A Y_{AZH} = A_0, \sum_{AZH} Z Y_{AZH} = Z_0, \sum_{AZH} H Y_{AZH} = H_0.$$

chemical potentials are from mass, charge and *H*yperon number conservations

$$F_{AH}^{hyp} = E_{sam}^{hyp} = H \cdot (-10.68 + 48.7/(A^{2/3})).$$

-- C.Samanta et al. J. Phys. G: 32 (2006) 363
(motivated: single Λ in potential well)

$$F_{AH}^{hyp} = (H/A) \cdot (-10.68A + 21.27A^{2/3}).$$

-- liquid-drop description of hyper-matter

A.S.Botvina and J.Pochodzalla, Phys. Rev.C76 (2007) 024909

Abundant hyper-isotope production in multifragmentation (SMM)

Important features of these reactions: wide fragment/isotope distributions

Statistical regularities of fragment production can be employed to learn about fragments!

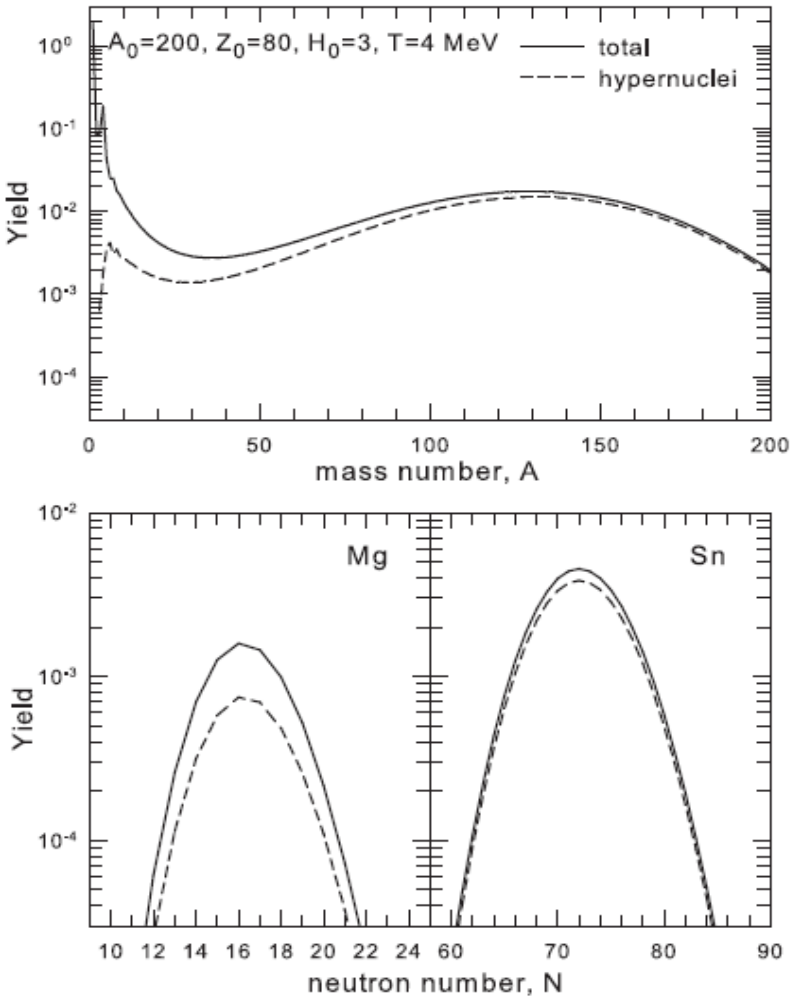

Yields of fragments: $$Y_{A,Z,H} = g_{A,Z,H} \cdot V_f \frac{A^{3/2}}{\lambda_T^3} \exp\left[-\frac{1}{T}\left(F_{A,Z,H} - \mu_{AZH}\right)\right],$$

$$\mu_{AZH} = A\mu + Z\nu + H\xi.$$

A mechanism for production of novel fragments: Capture of produced baryons by other nucleons and by spectator residues (nuclear matter)

Phenomenological models:

Coalescence (condensation) of baryons into clusters: **CB**

momenta:

$$|Pi - P0| \le Pc$$

coordinates:

$$|Xi - X0| \le Xc$$

Capture in nuclear potential and coalescence are similar mechanisms

Hyperon capture in the spectator potential

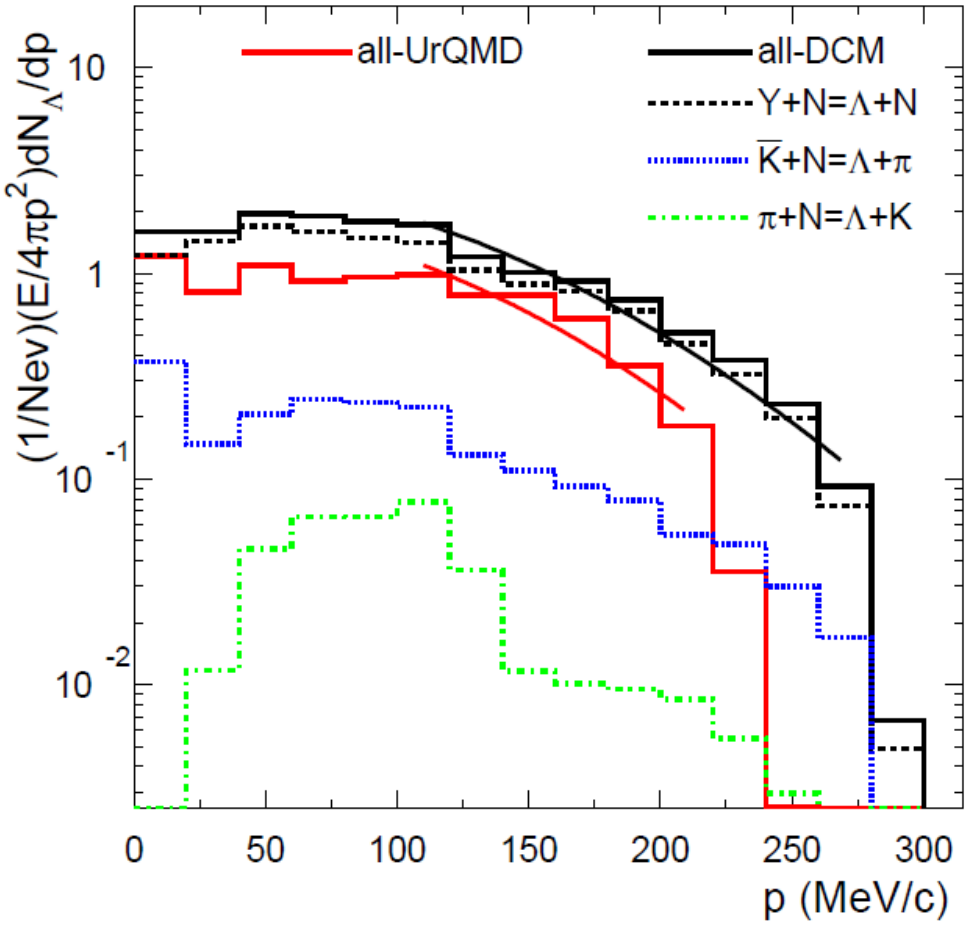

Au(20AGeV)+Au: UrQMD&DCM: PRC**84**, 064904 (2011)

Production of light nuclei in high energy central collisions

DCM, UrQMD, CB - Phys. Lett. B**714**, 85 (2012), Phys. Lett. B742, 7 (2015)

DCM versus experiment : coalescence mechanism

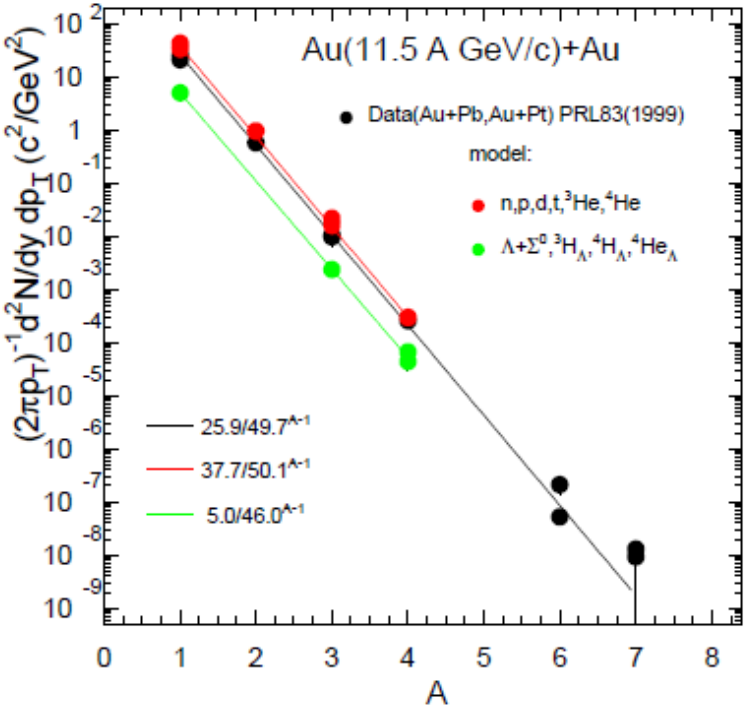

It is not possible to produce big nuclei !

Hybrid approach at LHC energies: UrQMD+hydrodynamics+coalescence

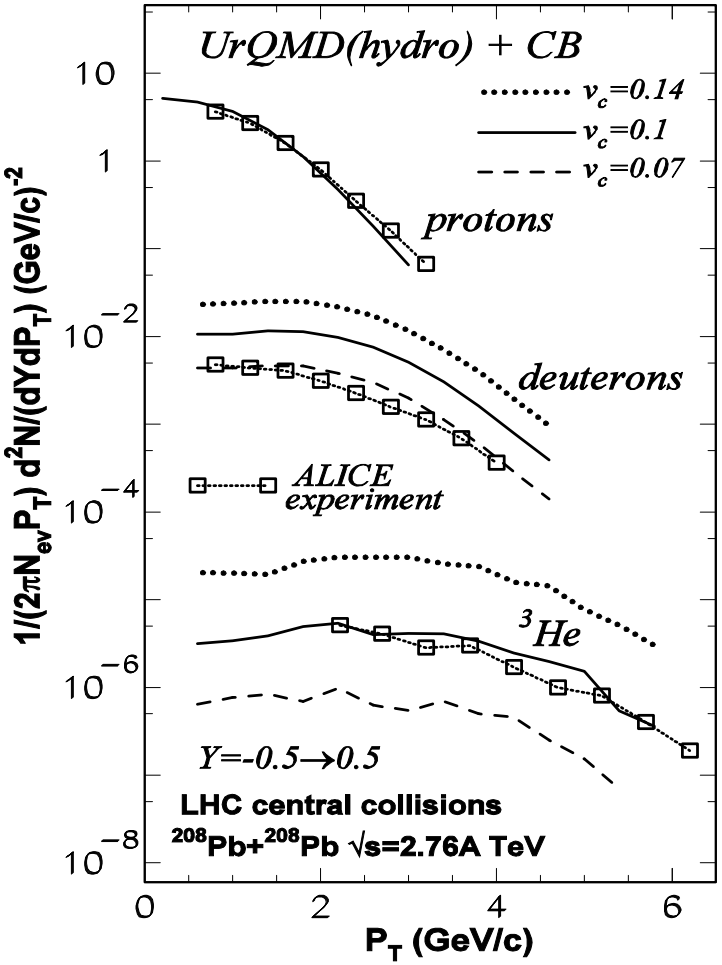

Phys. Rev. C96, 014913 (2017)

A.Botvina, J.Steinheimer, E.Bratkovskaya, M.Bleicher, J.Pochodzalla, PLB742(2015)7

normal- and hyper-fragments; hyper-residues @ target/projectile rapidities

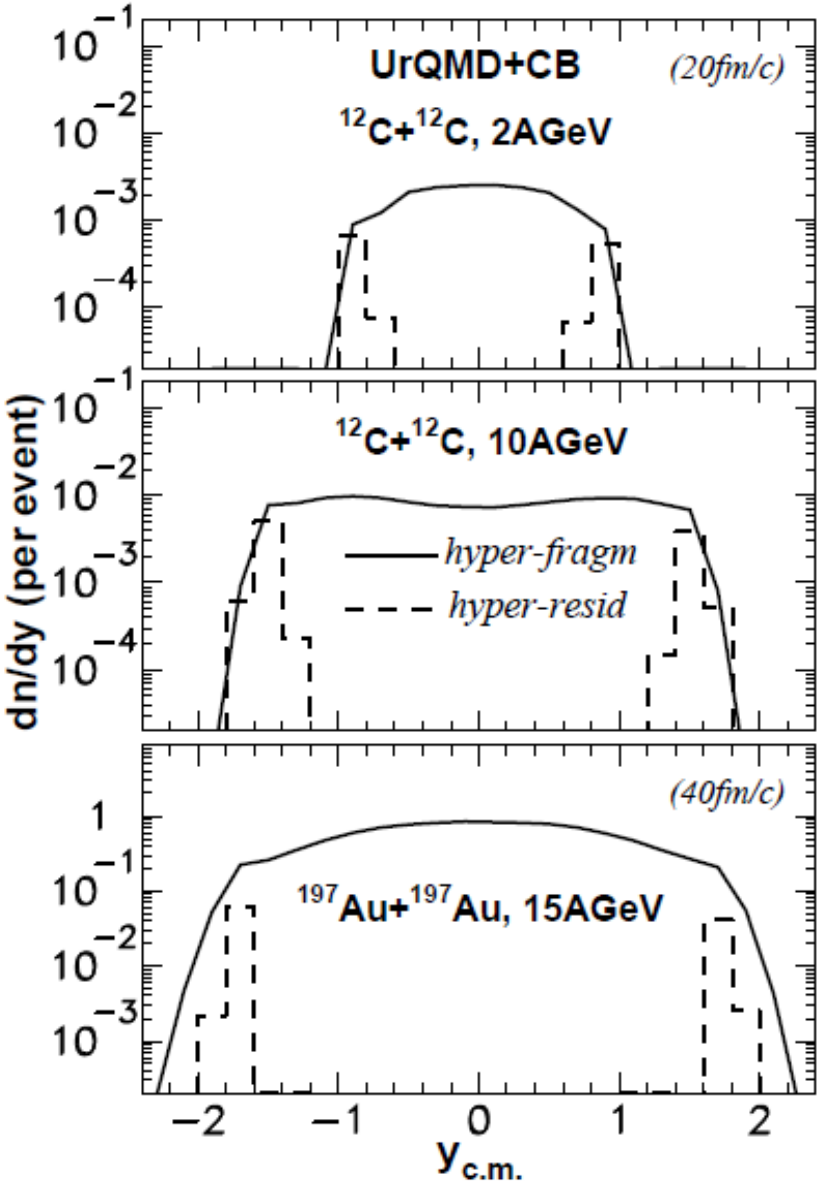

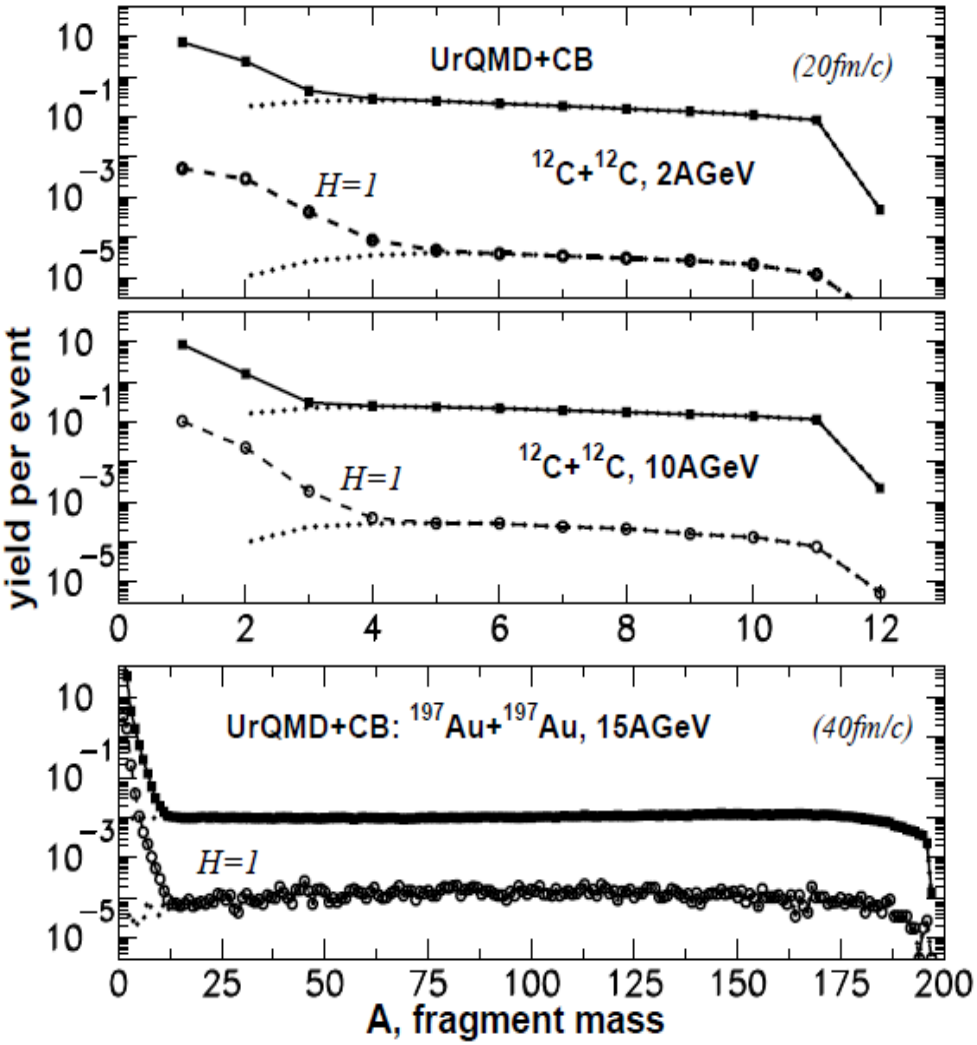

Because of secondary interactions the maximun of the fragments production is shifted from the midrapidity. Secondary products have relatively low kinetic energies, therefore, they can produce clusters and hypernuclei with higher probability.

for LHC @ 2.76 A TeV

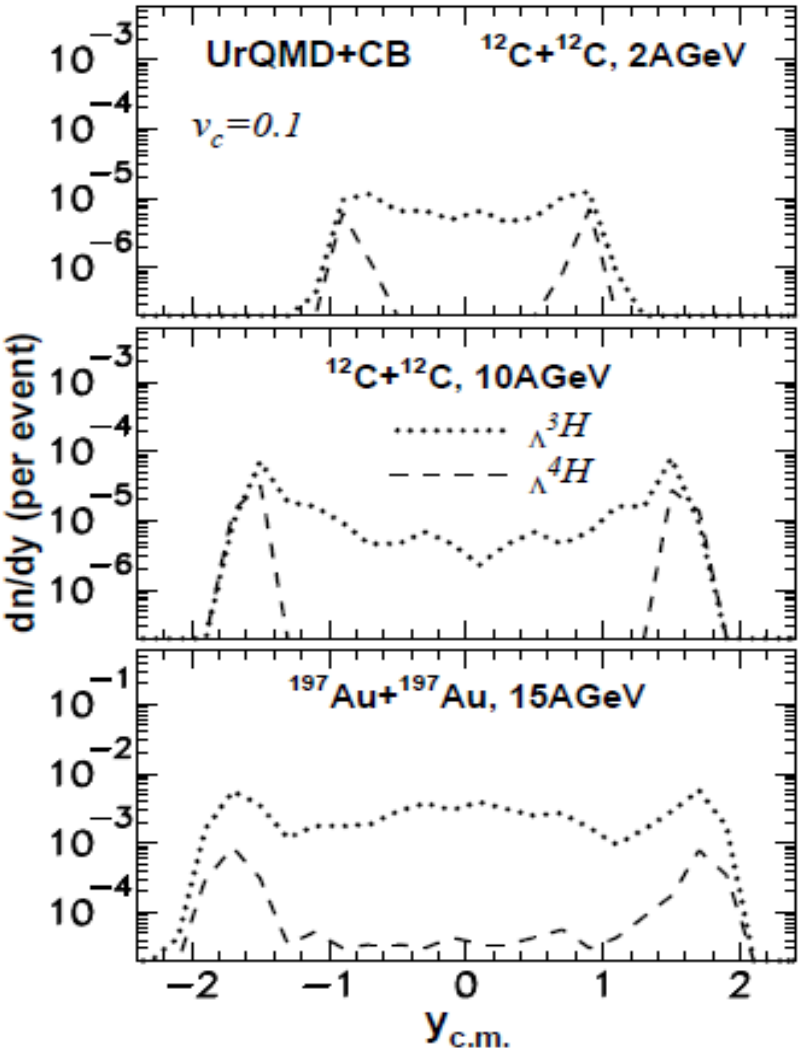

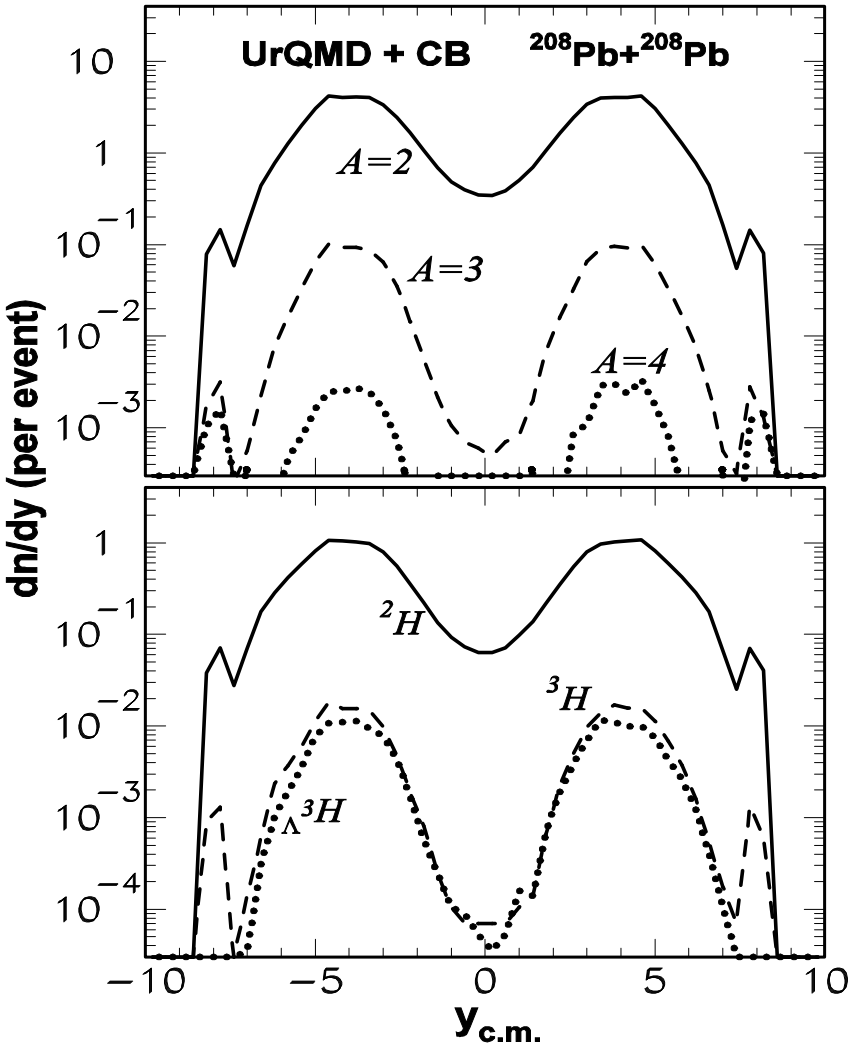

Novel: coalescent fragments can be excited & undergo de-excitation

De-excitation influences mass distributions: Examples for transport (DCM) + coalescence of baryons (CB) + statistical de-excitation (De) calculation. SMM is used.

Velocity coalescent parameter, **Vc=0.22 c** gives their excitation energies around ~10 MeV/nucl.

Final exponential-like decreasing of the mass yields with A.

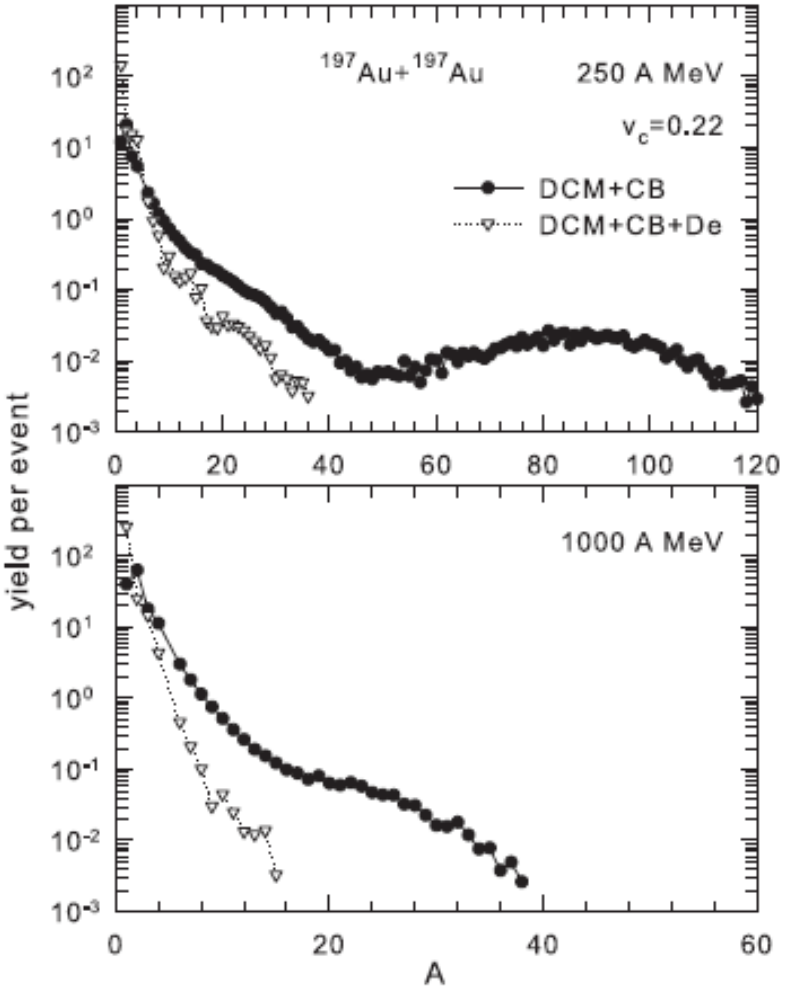

Novel: coalescent fragments can be excited & undergo de-excitation

De-excitation influences energy spectra. One can measure important correlations: the reaction mechanism can be established.

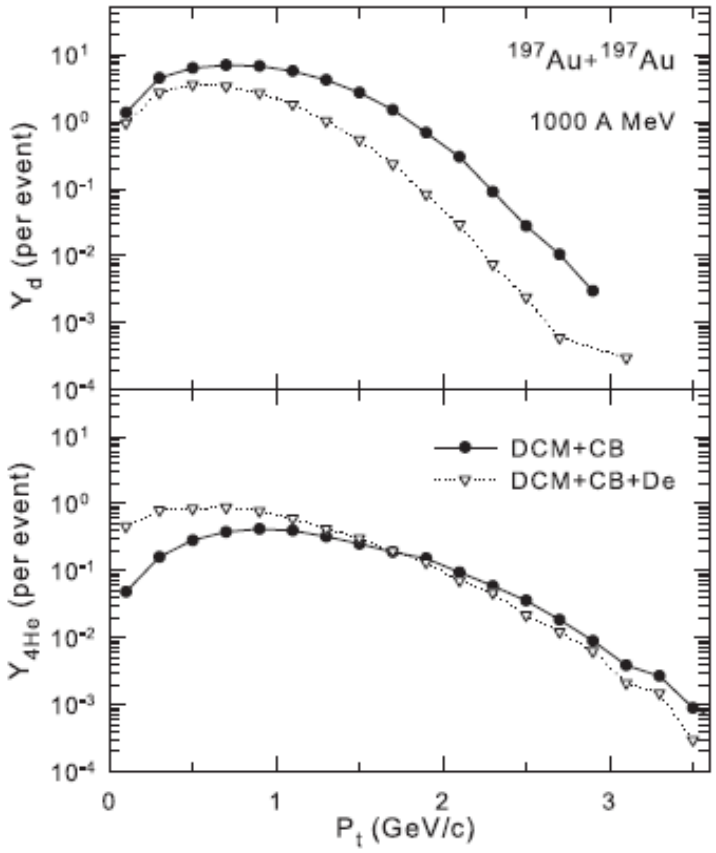

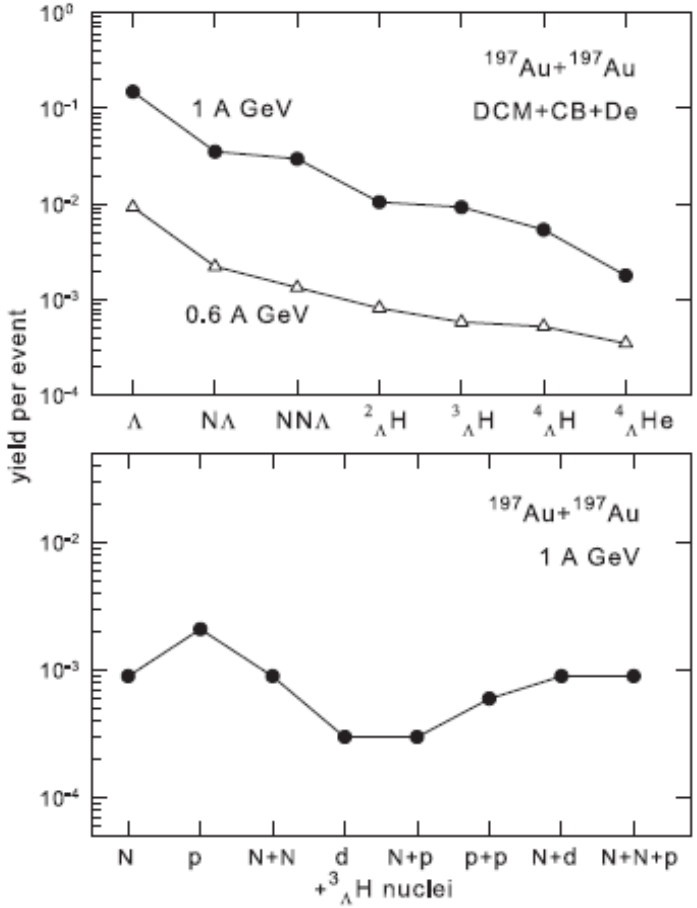

For special comparison with experiment (FOPI data , NPA**848**(2010)366) we perform the selection of central-isotropic events: DCM central event selection is not sufficient.

We suggest the isotropic phase space generation of nucleons in microcanonical approach (PSG) with the total available energy which can correspond to the c.m. energy of colliding nuclei. Also the isotropic hydrodynamical-like generation (HYG) can be involved.
(A.Botvina, N.Buyukcizmeci, M.Bleicher, PRC 103 (2021) 064602)

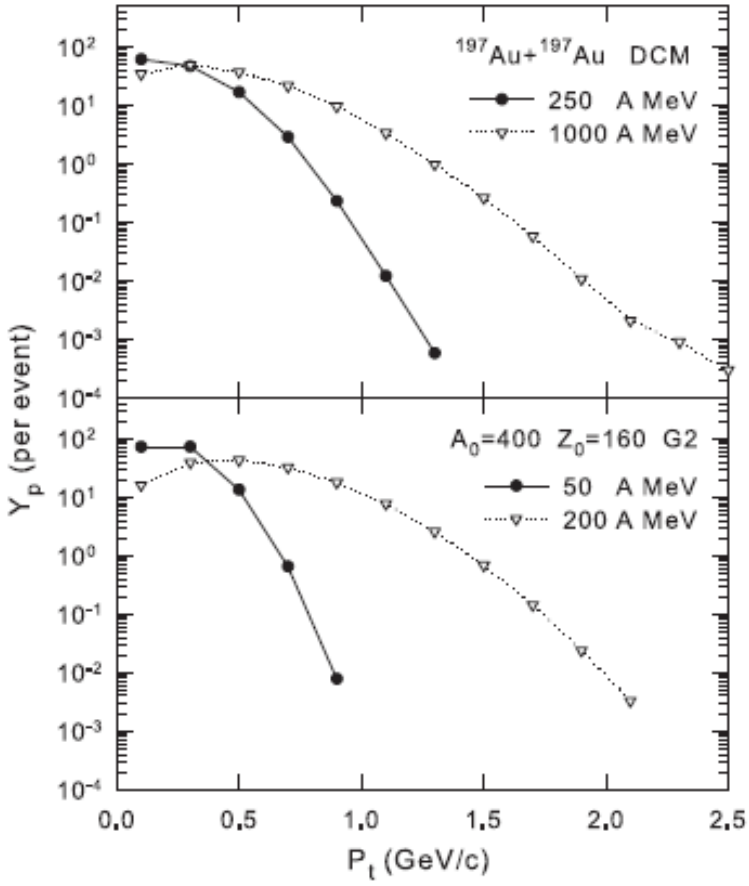

FIG. 16: Transverse momenta distributions of protons produced after the dynamical DCM stage in Au+Au central collisions at energies of 1000 A MeV and 250 A MeV (top panel), and after the phase space disintegration of sources with energies of 200 A MeV and 50 A MeV (bottom panel).

Multifragmentation in intermediate and high energy nuclear reactions

Experimentally established:

1) few stages of reactions leading to multifragmentation,
2) short time ~100fm/c for primary fragment production,
3) freeze-out density is around $0.1\rho_0$,
4) high degree of equilibration at the freeze-out,
5) primary fragments are hot.